Available online at www.sciencedirect.com
ScienceDirect
Journal of Sound and Vibration 306 (2007) 111–135
JOURNAL OF SOUND AND VIBRATION
www.elsevier.com/locate/jsvi

Use of particle filters in an active control algorithm for noisy nonlinear structural dynamical systems

R. Sajeeb, C.S. Manohar, D. Roy*

Structures Lab, Department of Civil Engineering, Indian Institute of Science, Bangalore 560012, India

Received 10 October 2006; received in revised form 15 May 2007; accepted 19 May 2007
Available online 6 July 2007

Abstract

The problem of active control of nonlinear structural dynamical systems, in the presence of both process and measurement noises, is considered. The focus of the study is on the use of particle filters for state estimation in feedback control algorithms for nonlinear structures, when a limited number of noisy output measurements are available. The control design is done using the state-dependent Riccati equation (SDRE) method. The stochastic differential equations (SDEs) governing the dynamical systems are discretized using explicit forms of Ito–Taylor expansions. The Bayesian bootstrap filter and that based on sequential important sampling (SIS) are employed for state estimation. The simulation results show the feasibility of using particle filters and SDRE techniques in control of nonlinear structural dynamical systems.
© 2007 Elsevier Ltd. All rights reserved.

1. Introduction

The concept of active structural control, since its introduction in 1972 [1], has been extensively used for control of civil engineering structures subjected to dynamic loads. The ability of the actively controlled structures to adapt themselves to the frequency characteristics of the excitation [2] makes it very attractive in the field of earthquake engineering. Excellent surveys of the state-of-the-art techniques and developments in this field are available in Refs. [3,4]. Most of the research in this field deals with control of linear structures. The real engineering structure is, however, typically nonlinear and therefore a successful implementation of control systems demands control algorithms which are capable of handling structural nonlinearity.

Different control schemes, such as feedback linearization, gain scheduling, sliding mode control and back stepping control are used in practice for control of nonlinear systems. The details of these methods can be found in Refs. [5,6]. A recently developed technique that has shown considerable promise is the nonlinear extension to the linear quadratic regulator (LQR) problem, called the state-dependent Riccati equation (SDRE) method. An overview of this method is available in Ref. [7]. In the SDRE method, the equations of motion are represented in a linear-like form, called the state-dependant coefficient (SDC) form that corresponds to the system matrices expressed explicitly as functions of the current state. A standard LQR

*Corresponding author. Tel.: +91 80 2293 3129; fax: +91 80 2360 0404.
E-mail address: royd@civil.iisc.ernet.in (D. Roy).

0022-460X/$ - see front matter © 2007 Elsevier Ltd. All rights reserved.
doi:10.1016/j.jsv.2007.05.043

problem can then be solved over each time step to design the state feedback control law. Indeed, most of the dynamical systems of engineering interest allow a direct parameterization of the equations of motion in the SDC form. However, systems, which do not admit a direct parameterization, may also be handled [8]. The parameterization is not unique and the control law is sub-optimal. It has been shown that there exists a representation such that the SDRE feedback produces the optimal control law [9]. The stability of the feedback control law resulting from the SDRE method is well studied [9–13]. Global asymptotic stability of a general nonlinear system can be achieved by tuning the weighing parameters of the cost function as function of states [10]. Although computationally intensive, the SDRE technique is found to be practicable for real-time control applications [11,14]. The availability of fast and efficient numerical algorithms for solving the SDRE makes the SDRE method suitable for field applications of real-time control systems [15]. The SDRE-based control design has received wide acceptance among researchers in different fields like, aerospace engineering [16–20], robotics [14] and bio-medical engineering [21]. However, the potential of this method in structural control problems appears not to have been explored yet.

To develop a control algorithm, to be implemented successfully in structural engineering applications, one has to consider important issues such as limitations of the mathematical model, and the difficulty in measuring all the state variables. Due to the size and complexity of many structures, mathematical models may not represent all aspects of their behavior. The uncertainty so introduced in the model (process noise) assumes great importance in control design, since the performance of the control design depends on the accuracy of the predicted response. Although considerable literature is available on the control of nonlinear structural systems [22–34], uncertainties in the model have not been generally considered except in a few studies [28,32–34]. Studies reported in Refs. [29–31] refer to the optimal control of nonlinear systems of interest in structural engineering. However, stochastic optimal control of nonlinear systems has been considered only in a very few studies [32–34]. A comprehensive review on the recent advances in the control of nonlinear stochastic systems is available in Ref. [35]. One important aspect of considerable relevance in structural control is the non-availability of the full states of the system. It is seldom feasible to measure all the states of the system that are required for the design of the control system. Measurements of a very few states, often contaminated by noise, are usually available. If the effect of noise is ignored, one can still design a control system, using the concept of direct output feedback control design [36]. But the resulting control will not be as effective as the state feedback control. A practical strategy for designing an efficient control system using the available noisy measurements would be to use a filter for estimating the states from the limited available responses and design a state feedback control via the estimated states. The separation principle in control theory allows one to handle the control design and filtering separately. Though the theory holds for linear systems [37] and possibly for a class of nonlinear systems [38–40], a generally applicable form of such a theory is not yet available for nonlinear systems [5]. It is nevertheless desirable to design the controller and state estimator separately, even in the absence of a rigorously established separation principle [41,42]. In the present study, the filtering and control strategies are designed separately with the implicit assumption that a separation theory holds.

One has to use an appropriate filter/state estimator to estimate the states that in turn serve as input to the feedback controller. For a linear system with Gaussian additive noises, the classical Kalman filter provides the optimal state estimator. For nonlinear state estimation, there are two main classes of methods, viz., those based on extended Kalman filter (EKF) and its variants [43,44], and, those based on Monte Carlo simulations, popularly known as the particle filters [45–50]. The current practice for estimating dynamic states of a nonlinear system, required for control applications, is to use the EKF [41,42,51]. The EKF, which uses a local linearization around the current state, does not account for the non-Gaussian nature of nonlinear system states, and, therefore, can approximately capture only the first two moments of the conditional probability density function (pdf) of the state. This may be contrasted with particle filters, wherein the conditional pdf is directly updated through a set of random particles with associated weights. Therefore, unlike the EKF, particle filters are far more versatile in handling system nonlinearity, non-Gaussian nature of response and even non-Gaussian nature of noises. Different versions of particle filters are discussed in the literature. Density-based Monte Carlo filter, Bayesian bootstrap filter and sequential important sampling (SIS)-based filter are some of them. A summary of the development of these filters can be found in Refs. [52,53]. Particle filters provide powerful tools in state estimation, system identification and control [54]. Recently, the potential of this technique has been demonstrated for system identification of nonlinear structural dynamical systems [53].

To the best of the authors' knowledge, the applicability of particle filters for state estimation in nonlinear structural control applications has not been explored yet. In the present work, we use particle filters for state estimation and control of a few typically nonlinear oscillators of interest in structural engineering. The example problems include a Duffing oscillator, a Van der Pol oscillator, and a three degree-of-freedom (3-dof) spring mass system with bilinear stiffness characteristics. The control strategy, designed using the SDRE method, uses the states estimated from a limited number of noisy measurements available. The governing stochastic differential equations (SDEs) of these oscillators are numerically integrated using explicit marching schemes based on the Ito–Taylor expansion, for processing in the filtering algorithm. The simulations are clearly indicative of the feasibility of particle filters and SDRE technique in control of nonlinear structural dynamical systems.

2. Problem description

By way of a general framework, consider a nonlinear dynamical system in the state space form as $\dot{x} = f(x, u)$, where $x(t, u) : \Re \times \Re^{n_u} \to \Re^{n_x}$ represents the state vector and $u \in \Re^{n_u}$ is the control force acting on the system. For notational convenience, we will often write $x(t, u)$ as $x(t)$ by dropping the argument u. The uncertainty in the system, arising from errors due to modeling and other sources, is assumed to admit a representation through Gaussian white noise processes. The governing equations therefore take the form of a system of SDEs. The white noise process, which is defined as the formal derivative of the Weiner process, only exists as a measure and not as a valid mathematical function. Hence, the governing SDEs are expressed in the following incremental form:

$$\mathrm{d}x(t) = \tilde{F}[x(t), u(t), t]\,\mathrm{d}t + \tilde{G}[x(t), t]\,\mathrm{d}B_I(t), \quad x(0) = x_0. \tag{1}$$

Here, $B_I(t) \in \Re^{m_I}$ is a standard vector Brownian motion process; $\tilde{F} : \Re^{n_x} \times \Re^{n_u} \times \Re \to \Re^{n_x}$ is the drift vector function, $\tilde{G} : \Re^{n_x} \times \Re \to \Re^{n_x \times m_I}$ is the diffusion coefficient matrix and $x_0 = x(t_0)$ is the initial condition vector, which may be deterministic or random with a known description. If one directly measures the state at a set of discrete time instants $\{t_k\}_{k=1}^{n_k}$, the measurement equation may be formally expressed as

$$y_k = \hat{H}_k(x_k) + \xi_k, \quad k = 1, 2, \ldots, n_k. \tag{2}$$

Here, $\xi_k \in \Re^{n_y}$ formally represents the vector of measurement noise. The objective is to determine the control force $u(t)$ so that a performance index of the form

$$J = \lim_{t_f \to \infty} \frac{1}{t_f} E\left\{ \int_0^{t_f} L[x(t), u(t), t]\,\mathrm{d}t \right\} \tag{3}$$

is minimized. Here $E[\cdot]$ represents the mathematical expectation operator and $L[\cdot]$ is a cost function whose definition would be made more precise later in the paper.

Since the focus of the present study is to demonstrate the use of particle filters in a structural control algorithm, the problem described through Eqs. (1)–(3) is not directly attempted here.

Assuming that the separation principle holds, one may tackle the output feedback control problem in two steps: (1) design a state feedback control law, assuming that the state $x(t)$ is available and (2) design a filter and replace x with the estimate $\hat{x}$ in the control law. Though, there is no general separation principle available for nonlinear systems, its validity is often assumed for all practical purposes. The controller-filter arrangement is schematically shown in Fig. 1. In the present study, we assume that the separation principle holds and design the controller and state estimator separately. A sub-optimal control law is designed using the SDRE method and the state estimation is done using a particle filter.

3. The control design using the SDRE method

The SDRE method, which is a nonlinear extension of the classical LQR control law, has received wide acceptance for control of nonlinear structures in recent years [14,16–21]. The details of this method can be found in Refs. [7,8]. The SDRE control design procedure is briefly outlined here. Here the governing equation of the nonlinear system $\dot{x} = f(x, u)$ is represented in a linear-like form, i.e., the SDC form with the system

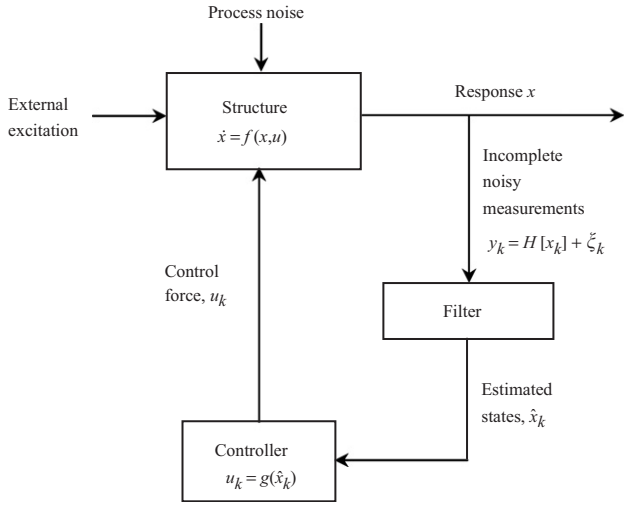

Fig. 1. A schematic diagram of the controller-filter arrangement.

matrices being explicit functions of the current state, as

$$\dot{x} = A(x)x + B(x)u. \tag{4}$$

For the system to be controllable, the matrices $A(x)$ and $B(x)$, evaluated at all possible states, should satisfy the controllability condition

$$\text{Rank}[B(x), \quad A(x)B(x), \quad A^2(x)B(x), \ldots, A^{n-1}(x)B(x)] = n, \tag{5}$$

where n is the size of the system matrix $A(x)$. A SDRE

$$A^{\mathrm{T}}(x)P(x) + P(x)A(x) - P(x)B(x)R^{-1}(x)B^{\mathrm{T}}(x)P(x) + Q(x) = 0 \tag{6}$$

is then formulated and solved for the symmetric, positive definite state-dependent matrix $P(x)$ to obtain the control law given by

$$u = -R^{-1}(x)B^{\mathrm{T}}(x)P(x)x. \tag{7}$$

The matrices $Q(x)$ and $R(x)$ are the weighing matrices in the performance index:

$$J = \frac{1}{2}\int_0^\infty \left(x^{\mathrm{T}}Q(x)x + u^{\mathrm{T}}R(x)u\right) \mathrm{d}t. \tag{8}$$

To ensure local stability, we require that $Q(x)$ is positive semi-definite and $R(x)$ positive definite. We can tune the weighing matrices $Q(x)$ and $R(x)$ appropriately to obtain the desired performance objectives. Note that, as the separation principle is assumed to hold in the present study, control design may be done in a deterministic framework. It is also worth noting that, in contrast to Eq. (3) that represents a general form of the performance index of a stochastic control problem, Eq. (8) refers to the standard form of a deterministic controller.

4. The state estimation using particle filters

A brief overview of the particle filters is provided in this section. In order to obtain estimates of the dynamic states, the SDEs representing the system dynamics/observations need to be numerically integrated through a discretized time-marching scheme. Thus consider a discretization of the form

$$x_{k+1} = f_k(x_k, w_k), \tag{9a}$$

$$y_k = h_k(x_k, v_k), \tag{9b}$$

where $f_k : \Re^{n_x} \times \Re^{n_w} \to \Re^{n_x}$ is a nonlinear function of the state $x_k \in \Re^{n_x}$ (with the subscript k denoting the time instant t_k), $h_k : \Re^{n_x} \times \Re^{n_v} \to \Re^{n_y}$ is a linear/nonlinear function of the state, $w_k \in \Re^{n_w}$ and $v_k \in \Re^{n_v}$ are zero-mean noise variables independent of current and past states and $y_k \in \Re^{n_y}$ is the instantaneous measurement vector. Since the vector sequence x_k is derived through a strong discretization of the governing SDEs, it follows that x_k possesses the strong Markov property and that the conditional pdfs $p(x_k|x_{k-1})$ and $p(y_k|x_k)$ are deducible from Eq. (9). For convenience, we introduce the following notations: $x_{0:k} := \{x_i\}_{i=0}^{k}$ and $y_{1:k} := \{y_i\}_{i=1}^{k}$. The objective is to determine the conditional pdf, $p(x_{0:k}|y_{1:k})$, which represents the pdf of the discretized state vectors conditioned on the observations available up to time t_k.

More specifically, we need to obtain the marginal pdf $p(x_k|y_{1:k})$, known as the filtering density, to estimate such statistical properties as conditional mean $\hat{x}_k$ and conditional covariance Σ_k given by

$$\hat{x}_k = E[x_k|y_{1:k}] = \int x_k p(x_k|y_{1:k})\,\mathrm{d}x_k, \tag{10a}$$

$$\Sigma_k = E[(x_k - \hat{x}_k)(x_k - \hat{x}_k)^{\mathrm{T}}] = \int (x_k - \hat{x}_k)(x_k - \hat{x}_k)^{\mathrm{T}} p(x_k|y_{1:k})\,\mathrm{d}x_k. \tag{10b}$$

The integrals in Eq. (10) are multidimensional in nature and their analytical evaluations are generally not possible. However, when the process and measurement equations are linear and the noises are Gaussian and additive, the Kalman filter provides the exact solution. For a more general case, a formal solution may be derived as follows [45]:

$$p(x_k|y_{1:k-1}) = \int p(x_k, x_{k-1}|y_{1:k-1})\,\mathrm{d}x_{k-1} = \int p(x_k|x_{k-1}) p(x_{k-1}|y_{1:k-1})\,\mathrm{d}x_{k-1}. \tag{11}$$

This equation represents the prediction equation. When the measurement vector y_k becomes available, one can derive the updation equation as follows:

$$p(x_k|y_{1:k}) = \frac{p(x_k, y_{1:k})}{p(y_{1:k})} = \frac{p(x_k, y_k, y_{1:k-1})}{p(y_k, y_{1:k-1})} = \frac{p(y_k|x_k) p(x_k|y_{1:k-1})}{p(y_k|y_{1:k-1})}. \tag{12}$$

Using the identity $p(y_k|y_{1:k-1}) = \int p(x_k, y_k|y_{1:k-1})\,\mathrm{d}x_k = \int p(y_k|x_k) p(x_k|y_{1:k-1})\,\mathrm{d}x_k$, the updation equation may further be expressed as

$$p(x_k|y_{1:k}) = \frac{p(y_k|x_k) p(x_k|y_{1:k-1})}{\int p(y_k|x_k) p(x_k|y_{1:k-1})\,\mathrm{d}x_k}. \tag{13}$$

Eqs. (11) and (13) constitute the formal solution to the estimation problem. The general principle of the particle filters is to use Monte Carlo simulation strategies to approximately obtain the above integrals. Different versions of particle filters such as density filter [46], Bayesian bootstrap filter [45], and SIS filters [48,49,52] are available in the literature. The density filter does not use a resampling scheme and hence, after a few time steps, the effective sample size reduces. Both Bayesian bootstrap filter and filter based on SIS density function uses some resampling strategies so that the samples get concentrated near regions of high probability densities. In the present study, we mainly employ the Bayesian bootstrap filter for state estimation owing to its simplicity and computational ease. However, we also use the filter based on SIS for comparison.

The formulation of the Bayesian bootstrap filter is based on an earlier result by Smith and Gelfand [55]. This result can be stated as follows. Let $\{x_k^*(i)\}_{i=1}^{N}$ be samples available from a continuous density function $G(x)$ (where the argument 'i' within the inner parenthesis represents the ith event). Moreover, suppose that we need samples from the pdf proportional to $L(x)G(x)$, where $L(x)$ is a known function. Then the theorem states that samples drawn from a discrete distribution over $\{x_k^*(i)\}_{i=1}^{N}$ with probability mass function $L(x_k^*(i)) \Big/ \sum_{j=1}^{N} L(x_k^*(j))$ on $x_k^*(i)$ tends in distribution to the required density as N tends to infinity. The algorithm for implementing the filter is as follows:

1. Set $k = 0$. Draw sample $\{x_0^*(i)\}_{i=1}^{N}$ from the pdf $p(x_0)$ and $\{w_0(i)\}_{i=1}^{N}$ from the pdf $p(w)$ of the noise.
2. Using the process Eq. (9a), obtain $\{x_k^*(i)\}_{i=1}^{N}$, $k > 0$, recursively.
3. When y_k arrives, find $p(y_k|x_{i,k}^*)$ and define $q_i = p(y_k|x_k^*(i)) \Big/ \sum_{j=1}^{N} p(y_k|x_k^*(j))$

4. Define the probability mass function $P[x_k(i) = x_k^*(i)] = q_i$ and generate samples $\{x_k^*(i)\}_{i=1}^N$ from this discrete distribution.
5. Estimate the conditional mean $\hat{x}_k \cong (1/N)\sum_{i=1}^N x_k(i)$ and conditional covariance $\Sigma_k \cong (1/(N-1))$ $\sum_{i=1}^N (x_k(i) - \hat{x}_k)(x_k(i) - \hat{x}_k)^{\mathrm{T}}$. The diagonal elements of Σ_k represent the variance associated with the estimated states.
6. With k replaced by $k+1$, repeat steps 2 through 5 till the terminal time is reached.

Using the result by Smith and Gelfand, if $G(x)$ is identified as $p(x_k|y_{1:k-1})$ and $L(x)$ as $p(y_k|x_k)$, one can see from the updation Eq. (14) that the samples $\{x_k(i)\}_{i=1}^N$, drawn in step 4 above, are approximately distributed as per the pdf $p(x_k|y_{1:k})$. In other words, the samples from the initial pdf $p(x_0)$ are propagated through the process equation and updated to represent samples from the filtering density.

If one uses the SIS filter, the estimate $\hat{x}_k$ may be obtained by rewriting Eq. (10a) as

$$\hat{x}_k = \int x_k \frac{p(x_k|y_{1:k})}{\pi(x_k|y_{1:k})}\pi(x_k|y_{1:k})\,\mathrm{d}x_k = \int x_k w^*(x_k)\pi(x_k|y_{1:k})\,\mathrm{d}x_k = E_\pi[x_k w^*(x_k)], \tag{14}$$

where $E_\pi[\cdot]$ stands for the expectation operator defined with respect to the pdf $\pi(x_k|y_{1:k})$ and $w^*(x_k) = p(x_k|y_{1:k})/\pi(x_k|y_{1:k})$. Obtaining the optimal importance sampling density function is not an easy task. However, when the process and measurement equations assume the form

$$x_k = f(x_{k-1}) + v_k; \quad v_k \sim N[\,0_{n_v\times 1} \quad \Sigma_v\,], \tag{15a}$$

$$y_k = Cx_k + w_k; \quad w_k \sim N[\,0_{n_w\times 1} \quad \Sigma_w\,] \tag{15b}$$

the optimal importance density function is shown to be a normal density function with mean m_k and covariance Σ given by

$$m_k = \Sigma\left(\Sigma_v^{-1} f(x_{k-1}) + C^{\mathrm{T}}\Sigma_w^{-1} y_k\right), \tag{16a}$$

$$\Sigma^{-1} = \Sigma_v^{-1} + C^{\mathrm{T}}\Sigma_w^{-1} C. \tag{16b}$$

When the effective sample size at any time instant falls below a threshold (N_{thres}), a resampling is performed to counter an impoverishment of samples. The algorithm for implementing the SIS filter is available in Refs. [49,52,53] and is skipped here for conciseness.

Theoretically, the estimate through the particle filter approaches the exact solution, as the number of samples N tends to infinity. It is therefore of interest to study the performance of the particle filter with different sample sizes, especially for a linear system with Gaussian additive noises—a problem for which the exact solution is available through the Kalman filter. For a linear single degree of freedom (sdof) system subjected to a harmonic load, the variance associated with the estimates of velocity using Kalman filter and particle filter (bootstap filter) with different ensemble sizes is shown in Fig. 2; the caption to this figure provides the details of the system parameters considered. It is readily observable that the particle filter estimate approaches the Kalman filter estimate as N increases.

5. The discretization of the system/observation equations

5.1. The discretization

The governing SDEs for the system/observations need to be discretized and brought to a form consistent with Eqs. (9a) and (9b) and this enables further processing with the filtering algorithm. Just as a time-marching algorithm for a deterministic ODE is often derived using variations of a Taylor expansion, the SDEs may similarly be discretized using the stochastic Taylor (Ito–Taylor) expansion [56,57]. Details of Ito–Taylor expansion and related concepts of stochastic calculus may be found in Refs. [53,56–58]. However, a brief overview of the stochastic Taylor expansion is provided in the Appendix.

In the present study, we consider three nonlinear oscillators, namely, two sdof and a 3-dof oscillators. While the sdof oscillators are the Duffing oscillator with a cubic stiffness term and the Van der Pol (VDP) oscillator

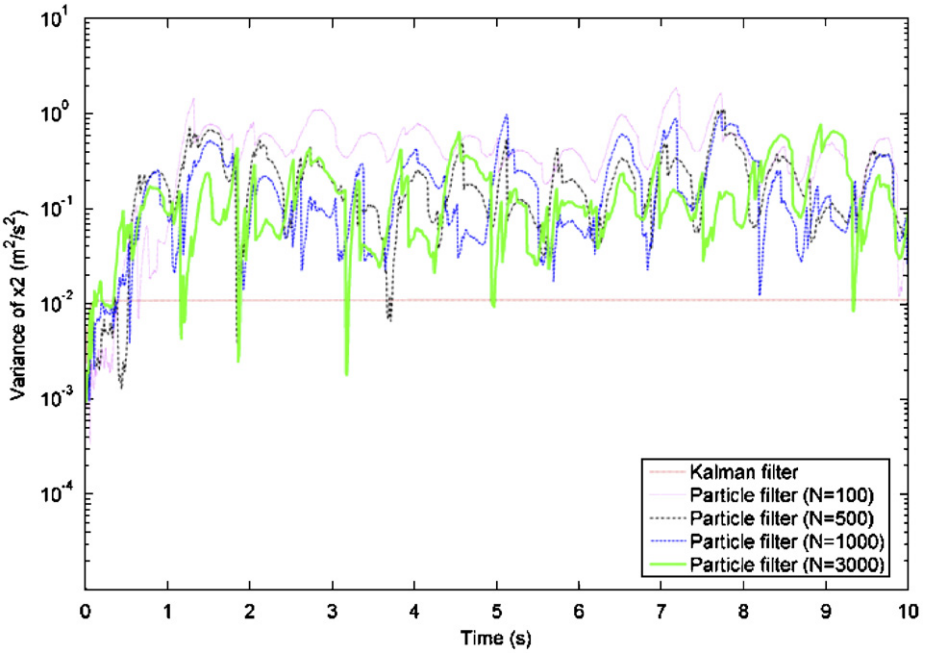

Fig. 2. Performance of particle filter with different sample size. Here, a linear sdof system given by $m\ddot{x} + c\dot{x} + \alpha x = P_0 \cos \lambda t$ is considered. Initial condition: $x(0) = \dot{x}(0) = 0$. System parameters are: $m = 1$ kg, $c = 0.5$ N s/m, $\alpha = 10$ N/m, $P_0 = 5$ N and $\lambda = 5$ rad/s. Process noise parameter $\sigma = 0.05P_0$ and standard deviation of measurement noise is 0.25. The filter estimates the states x_1 (displacement) and x_2 (velocity) from the noisy measurement of x_2.

with a nonlinear damping term, the nonlinearity in the 3-dof oscillator arises due to bilinear springs (Fig. 3). The forces $u_1(t)$, $u_2(t)$ and $u_3(t)$ acting in the model may be interpreted as control forces. The governing equations of motion of the sdof Duffing and VDP oscillators, both subjected to support motions, are, respectively, of the following forms:

$$m\ddot{x} + c\dot{x} + \alpha x + \beta x^3 = u(t) - m\ddot{x}_g, \quad x(0) = x_0, \quad \dot{x}(0) = \dot{x}_0, \tag{17}$$

$$m\ddot{x} - \mu(1 - x^2)\dot{x} + \alpha x = u(t) - m\ddot{x}_g, \quad x(0) = x_0, \quad \dot{x}(0) = \dot{x}_0, \tag{18}$$

where $u(t)$ is the control force and x is the relative displacement of the mass point with respect to the support. Referring to Fig. 3(a), the equations of motion of the 3-dof spring-mass system, again under support motion, may be expressed as

$$m_1\ddot{x}_1 + (c_1 + c_2)\dot{x}_1 - c_2\dot{x}_2 + fs_1(x_1) + fs_2(x_1 - x_2) = -m_1\ddot{x}_g + u_1(t), \tag{19a}$$

$$m_2\ddot{x}_2 - c_2\dot{x}_1 + (c_2 + c_3)\dot{x}_2 - c_3\dot{x}_3 + fs_2(x_2 - x_1) + fs_3(x_2 - x_3) = -m_2\ddot{x}_g + u_2(t), \tag{19b}$$

$$m_3\ddot{x}_3 - c_3\dot{x}_2 + c_3\dot{x}_3 + fs_3(x_3 - x_2) = -m_3\ddot{x}_g + u_3(t) \tag{19c}$$

with initial conditions $x_1(0) = x_{10}$, $x_2(0) = x_{20}$, $x_3(0) = x_{30}$, $\dot{x}_1(0) = \dot{x}_{10}$, $\dot{x}_2(0) = \dot{x}_{20}$ and $\dot{x}_3(0) = \dot{x}_{30}$. x_1, x_2 and x_3 are, respectively, the relative displacements of the mass points m_1, m_2 and m_3 with respect to the support.

The SDEs corresponding to the Duffing oscillator (Eq. (17)), after incorporating the process noise, may be expressed in the following incremental form:

$$\mathrm{d}x_1 = x_2\,\mathrm{d}t, \tag{20a}$$

$$\mathrm{d}x_2 = \left\{\frac{1}{m}\left(-\alpha x_1 - \beta x_1^3 - cx_2 + u(t)\right) - \ddot{x}_g\right\}\mathrm{d}t + \sigma_d\,\mathrm{d}B_1. \tag{20b}$$

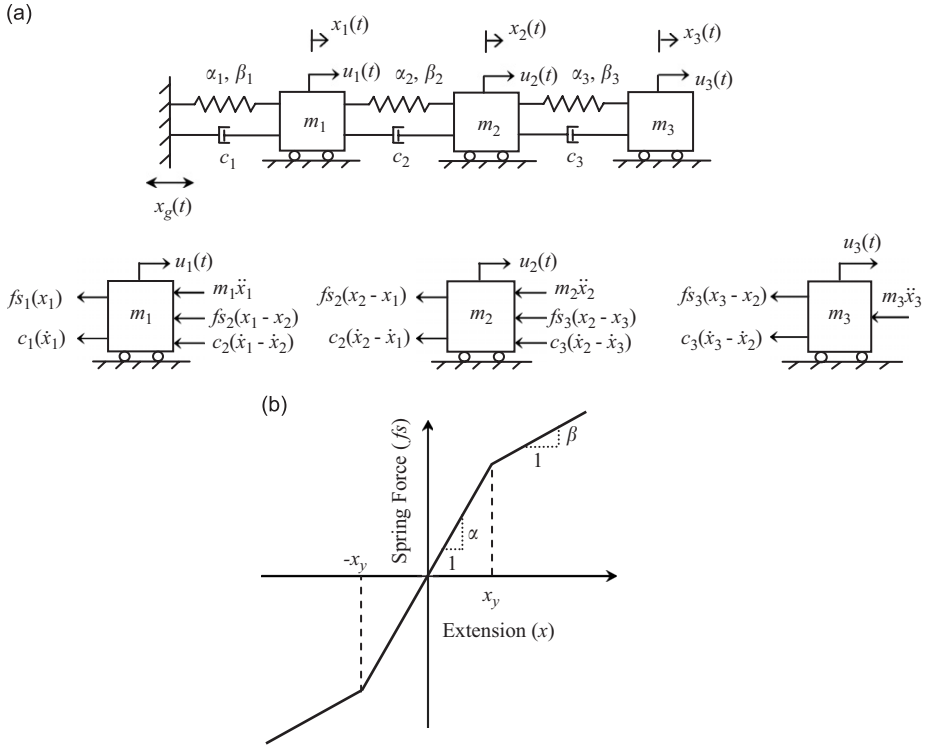

Fig. 3. (a) 3-dof spring–mass system with bilinear spring (x_1, x_2 and x_3 represent the relative displacement with respect to the support) and (b) force-displacement relation of the bilinear spring.

For the VDP oscillator, the SDEs in an incremental form are given by

$$\mathrm{d}x_1 = x_2\,\mathrm{d}t, \tag{21a}$$

$$\mathrm{d}x_2 = \left\{\frac{1}{m}[(-\alpha x_1 + \mu(1 - x_1^2)x_2 + u(t)] - \ddot{x}_g\right\}\mathrm{d}t + \sigma_v\,\mathrm{d}B_1. \tag{21b}$$

Similarly, the SDEs representing the 3-dof spring-mass system are

$$\mathrm{d}x_1 = x_4\,\mathrm{d}t, \tag{22a}$$

$$\mathrm{d}x_2 = x_5\,\mathrm{d}t, \tag{22b}$$

$$\mathrm{d}x_3 = x_6\,\mathrm{d}t, \tag{22c}$$

$$\mathrm{d}x_4 = \left\{-\frac{1}{m_1}[(c_1 + c_2)x_4 - c_2x_5 + fs_1(x_1) + fs_2(x_1 - x_2)] - \ddot{x}_g + \frac{u_1(t)}{m_1}\right\}\mathrm{d}t + \sigma_1\,\mathrm{d}B_1, \tag{22d}$$

$$\mathrm{d}x_5 = \left\{-\frac{1}{m_2}[-c_2x_4 + (c_2 + c_3)x_5 - c_3x_6 + fs_2(x_2 - x_1) + fs_3(x_2 - x_3)] - \ddot{x}_g + \frac{u_2(t)}{m_2}\right\}\mathrm{d}t + \sigma_2\,\mathrm{d}B_2, \tag{22e}$$

$$\mathrm{d}x_6 = \left\{-\frac{1}{m_3}[-c_3x_5 + c_3x_6 + fs_3(x_3 - x_2)] - \ddot{x}_g + \frac{u_3(t)}{m_3}\right\}\mathrm{d}t + \sigma_3\,\mathrm{d}B_3. \tag{22f}$$

The coefficients σ_d, σ_v, σ_1, σ_2 and σ_3 in the above equations measure intensities of the associated additive noise processes; for instance, a zero value for these quantities implies a purely deterministic model.

Using the procedure outlined in the Appendix, we can write explicit forms of stochastic Taylor expansion for the displacement and velocity components of the dynamical systems considered over the interval $(t_k, t_{k+1}]$

with a uniform step-size $h = t_{k+1} - t_k$. Thus, for the Duffing oscillator (Eq. (20)), the maps for the displacement and velocity updates can be shown to be:

$$x_{1(k+1)} = x_{1k} + x_{2k}h + \sigma_d I_{10} + a_{2k}\frac{h^2}{2} - \frac{c}{m}\sigma_d I_{100} - (\ddot{x}_{g_k} - \ddot{x}_{g_{(k-1)}})\frac{h^2}{6} + \frac{1}{m}(u_k - u_{(k-1)})\frac{h^2}{6} - \frac{x_{2k}}{m}(\alpha + 3\beta x_{1k}^2)\frac{h^3}{6} - \frac{c}{m}a_{2k}\frac{h^3}{6} + \rho_{1k}, \tag{23a}$$

$$x_{2(k+1)} = x_{2k} - \frac{\alpha}{m}\left(x_{1k}h + x_{2k}\frac{h^2}{2}\right) - \frac{\beta}{m}\left(x_{1k}^3 h + 3x_{1k}^2 x_{2k}\frac{h^2}{2}\right) - \frac{c}{m}\left(x_{2k}h + a_{2k}\frac{h^2}{2}\right) - \frac{c}{m}\sigma_d I_{10} - \left(\frac{\ddot{x}_{g_{(k+1)}} + \ddot{x}_{g_k}}{2}\right)h + \frac{1}{m}\left(\frac{u_{(k+1)} + u_k}{2}\right)h + \sigma_d I_1 + \rho_{2k}, \tag{23b}$$

where

$$a_{2k} = \frac{1}{m}(-\alpha x_{1k} - \beta x_{1k}^3 - c x_{2k} + u_k) - \ddot{x}_{g_k}$$

and I_1, I_{10} and I_{100} are the MSIs given by

$$I_1 = \int_{t_k}^{t_{k+1}} \mathrm{d}B_1, \quad I_{10} = \int_{t_k}^{t_{k+1}}\int_{t_k}^{s} \mathrm{d}B_1\,\mathrm{d}s_1 \quad \text{and} \quad I_{100} = \int_{t_k}^{t_{k+1}}\int_{t_k}^{s}\int_{t_k}^{s_1} \mathrm{d}B_1\,\mathrm{d}s_1\,\mathrm{d}s_2. \tag{24}$$

Note that ρ_{1k} and ρ_{2k} are the remainder terms associated with the displacement and velocity maps, respectively. For computational purposes, these maps are then approximately given by Eq. (23) without including the remainder terms. It may be noted that the MSIs are denoted by I followed by a set of (non-negative) integer subscripts indicating the scalar components of Wiener increments in the same order as they appear within the integrals and integration with respect to time is indicated by a zero subscript. These MSIs are martingales and, if interpreted as Ito integrals, they are zero-mean Gaussian random variables. For the numerical implementation of the stochastic maps so obtained, one needs to generate realizations of these MSIs which, in turn, requires the knowledge of their covariance matrix. We derive the covariance matrix of I_1, I_{10} and I_{100} in Section 5.2. A similar discretization procedure may be applied to obtain the discrete maps for displacement and velocity components of the VDP oscillator.

Before applying the discretization procedure to the SDEs of the 3-dof oscillator, we need to write down a piecewise smooth expression for the forces in the bilinear springs. Thus, referring to Fig. 3(b), the force in the ith bilinear spring may be written as

$$fs_i(x_i) = \begin{cases} \alpha_i x_{y,i} + \beta_i(x_i - x_{y,i}) & \text{if } x_i > x_{y,i}, \\ \alpha_i x_i & \text{if } |x_i| \leqslant x_{y,i}, \\ -\alpha_i x_{y,i} + \beta_i(x_i - x_{y,i}) & \text{if } x_i < -x_{y,i}. \end{cases} \tag{25}$$

Eq. (25) can be generalized as

$$fs_i(x_i) = p_i(Q_i^y + \beta_i x_i) + q_i\alpha_i x_i + r_i(-Q_i^y + \beta_i x_i), \tag{26}$$

where $Q_i^y = (\alpha_i - \beta_i)x_{y,i}$ and p_i, q_i and r_i are given by $p_i = 1$, $q_i = r_i = 0$ if $x_i > x_{y,i}$; $q_i = 1$, $p_i = r_i = 0$ if $|x_i| \leqslant x_{y,i}$ and $r_i = 1$, $p_i = q_i = 0$ otherwise.

We may replace the spring forces in the governing SDEs of Eq. (22) by the RHS of Eq. (26). Now, following the discretization procedure, we may obtain stochastic Taylor expansions for the displacements and velocity components. The displacement and velocity maps for the first degree-of-freedom

may be shown to be:

$$x_{1(k+1)} = x_{1k} + x_{4k}h + a_{4k}\frac{h^2}{2} - \frac{1}{m_1}\left[(p_1\beta_1 + q_1\alpha_1 + r_1\beta_1 + p_2\beta_2 + q_2\alpha_2 + r_2\beta_2)x_{4k} - (p_2\beta_2 + q_2\alpha_2 + r_2\beta_2)x_{5k} + (c_1 + c_2)a_{4k} - c_2a_{5k}\right]\frac{h^3}{6} - \left(\ddot{x}_{g_k} - \ddot{x}_{g_{(k-1)}}\right)\frac{h^2}{6} + \frac{1}{m_1}\left(u_{1k} - u_{1(k-1)}\right)\frac{h^2}{6} + \sigma_1 I_{10} - \frac{1}{m_1}[(c_1 + c_2)\sigma_1 I_{100} - c_2\sigma_2 I_{200}], \tag{27a}$$

$$x_{4(k+1)} = z_{4k} - \frac{1}{m_1}\left[(c_1 + c_2)\left(x_{4k}h + a_{4k}\frac{h^2}{2}\right) - c_2\left(x_{5k}h + a_{5k}\frac{h^2}{2}\right) + (p_1 - r_1)Q_1^y h + (r_2 - p_2)Q_2^y h + (p_1\beta_1 + q_1\alpha_1 + r_1\beta_1 + p_2\beta_2 + q_2\alpha_2 + r_2\beta_2)\left(x_{1k}h + x_{4k}\frac{h^2}{2}\right) - (p_2\beta_2 + q_2\alpha_2 + r_2\beta_2)\left(x_{2k}h + a_{5k}\frac{h^2}{2}\right)\right] - \left(\frac{\ddot{x}_{g_{(k+1)}} + \ddot{x}_{g_k}}{2}\right)h + \frac{1}{m_1}\left(\frac{u_{1(k+1)} + u_{1k}}{2}\right)h + \sigma_1 I_1 - \frac{1}{m_1}[(c_1 + c_2)\sigma_1 I_{10} - c_2\sigma_2 I_{20}], \tag{27b}$$

where

$$a_{4k} = -\frac{1}{m_1}[(c_1 + c_2)x_{4k} - c_2x_{5k} + fs_1(x_{1k}) + fs_2(x_{1k} - x_{2k})] - \ddot{x}_{g_k} + \frac{u_1(t)}{m_1}$$

and

$$a_{5k} = -\frac{1}{m_2}[-c_2x_{4k} + (c_2 + c_3)x_{5k} - c_3x_{6k} + fs_2(x_{2k} - x_{1k}) + fs_3(x_{2k} - x_{3k})] - \ddot{x}_{g_k} + \frac{u_2(t)}{m_2}.$$

The stochastic Taylor expansions for displacement and velocity components corresponding to the other degrees-of-freedom may be obtained in a similar way.

The MSIs I_1, I_2 and I_3 are stochastically independent, zero-mean normal random variables with variance h. We also note that the above expansions assume that the vector field is adequately differentiable—a condition that is not met by $fs_i(x_i)$ (see Eq. (26)) whenever the event $x_i = x_{y,i}$ occurs. Even though this event has a measure zero of occurrence, its occurrence should ideally be detected when the solutions are in the strong form. However, an accurate detection of such events in the solutions of SDEs is still an open research problem and is beyond the scope of this study. It must be noted that, in neglecting the non-differentiability, the local error within a close neighborhood of the time of the event as well as the global error would get affected. However, local errors away from the point of discontinuity would remain unaffected. Moreover, for sufficiently small h, it is conjectured that the global error would not get significantly affected.

We observe that evaluations of the velocity components through the discretized maps at instant t_{k+1} require information on u_{k+1}, which is not known. Therefore, its value has to be extrapolated from the known values of u, available up to the instant t_k. A truncated Taylor expansion may readily be used to approximately obtain u_{k+1} as

$$u_{k+1} = u_k + \dot{u}_k h. \tag{28}$$

In Eq. (28), a dot over u_k represents, formally, the time rate of u evaluated at t_k and it is computed as $\dot{u}_k = (u_k - u_{(k-1)})/h$. Since the state of the system is presently being measured, the observation equation is in a discrete form: $y_k = h_k(x_k) + v_k$, where v_k is the vector of measurement noise.

5.2. Modeling the MSIs

Using Ito's formula, restricted to the interval $(t_k,\ t_{k+1}]$, the elements of the covariance matrix of the MSIs may be obtained. Consider the MSIs I_1, I_{10} and I_{100} (Eq. (24)). Let $x = I_1$, $y = I_{10}$ and $z = I_{100}$.

From Eq. (24), one gets:

$$\mathrm{d}x = \mathrm{d}B_1, \quad \mathrm{d}y = x\,\mathrm{d}t \quad \text{and} \quad \mathrm{d}z = y\,\mathrm{d}t. \tag{29}$$

We know that $E[I_1] = E[I_{10}] = E[I_{100}] = 0$ and $E[I_1^2] = h$. Consider the SDE $\mathrm{d}(xy) = x^2\,\mathrm{d}t + y\,\mathrm{d}B_1$. Therefore, $\mathrm{d}(E[xy]) = E(x^2)\,\mathrm{d}t$ or,

$$E[xy] = E[I_1, I_{10}] = \int_{t_k}^{t_{k+1}} E(x^2)\,\mathrm{d}t = \frac{h^2}{2}. \tag{30}$$

Now, consider the SDE $\mathrm{d}(xz) = xy\,\mathrm{d}t + z\,\mathrm{d}B_1$, so that $\mathrm{d}(E[xz]) = E(xy)\,\mathrm{d}t$ or,

$$E[xz] = E[I_1, I_{100}] = \int_{t_k}^{t_{k+1}} E(xy)\,\mathrm{d}t = \frac{h^3}{6}. \tag{31}$$

Moreover, from $\mathrm{d}(y^2) = 2xy\,\mathrm{d}t$, we have $\mathrm{d}(E[y^2]) = 2E(xy)\,\mathrm{d}t$. This leads to

$$E[y^2] = E[I_{10}^2] = 2\int_{t_k}^{t_{k+1}} E(xy)\,\mathrm{d}t = \frac{h^3}{3}. \tag{32}$$

Similarly, use of the SDE $\mathrm{d}(yz) = y^2\,\mathrm{d}t + xz\,\mathrm{d}t$ leads to

$$E[yz] = E[I_{10}, I_{100}] = \int_{t_k}^{t_{k+1}} E(y^2)\,\mathrm{d}t + \int_{t_k}^{t_{k+1}} E(xz)\,\mathrm{d}t = \frac{h^4}{8}. \tag{33}$$

From $\mathrm{d}(z^2) = 2yz\,\mathrm{d}t$, we get

$$E[z^2] = E[I_{100}^2] = 2\int_{t_k}^{t_{k+1}} E(yz)\,\mathrm{d}t = \frac{h^5}{20}. \tag{34}$$

Thus, we observe that these MSIs are normal random variables of the form

$$\begin{Bmatrix} I_1 \\ I_{10} \\ I_{100} \end{Bmatrix} \sim N\left[0_{3\times 1} \quad \begin{bmatrix} h & \frac{h^2}{2} & \frac{h^3}{6} \\ \frac{h^2}{2} & \frac{h^3}{3} & \frac{h^4}{8} \\ \frac{h^3}{6} & \frac{h^4}{8} & \frac{h^5}{20} \end{bmatrix} \right]. \tag{35}$$

6. Numerical illustrations

We now illustrate the control methodology with the two sdof and the 3-dof nonlinear oscillators as described earlier. Whilst the Duffing and VDP oscillators are typically workhorse nonlinear systems of general engineering interest, the 3-dof oscillator is a model, frequently encountered in earthquake engineering. The excitations in the sdof oscillators are in the form of harmonic support displacement, whereas for the 3-dof oscillator, an earthquake like support motion is considered. In most of the illustrations the structures are assumed to start from rest. The equations of motion of these structures are given (in Section 5) (see Eqs. (17)–(19)). The discretized forms of the SDEs resulting from these equations (following the introduction of process noises) have already been derived in the previous section.

We have presently considered the following parameter values for the Duffing oscillator: $m = 1\,\mathrm{kg}$, $c = 0.5\,\mathrm{N\,s/m}$, $\alpha = 10\,\mathrm{N/m}$ and $\beta = 5000\,\mathrm{N/m^3}$. The process noise parameter $\sigma_d = 0.01|\ddot{x}_g|_{\max}$ is assumed. For the VDP oscillator, we choose the system parameters as: $m = 1\,\mathrm{kg}$, $\alpha = 10\,\mathrm{N/m}$ and $\mu = 2\,\mathrm{N\,s/m^3}$. The noise parameter is taken as $\sigma_v = 0.01|\ddot{x}_g|_{\max}$. Finally, we choose the following parameter values for the 3-dof spring-mass system: $m_1 = m_2 = m_3 = 10\,\mathrm{kg}$ and $c_1 = c_2 = c_3 = 5\,\mathrm{N\,s/m}$. The stiffnesses corresponding to the two piecewise linear regimes of the bilinear springs are assumed as $\alpha_1 = \alpha_2 = \alpha_3 = 3000\,\mathrm{N/m}$ and

$\beta_1 = \beta_2 = \beta_3 = 750\,\mathrm{N/m}$. The critical displacements ($x_{y,i}$ $i = 1, 2, 3$) corresponding to the common point (henceforth called the critical point in the force-displacement space) of the two linear arms of the springs are taken to be 0.01 m and, the noise parameters are assumed as $\sigma_i = 0.01|\ddot{x}_g|_{\max}$ $(i = 1, 2, 3)$. For all cases, the standard deviation of measurement noise is assumed to be 6% of the maximum absolute value of the measured response quantity under noise free conditions. During simulations, the initial conditions are assumed to be deterministic. Considering small displacements, the natural frequency of the linear models of the sdof oscillators (obtained by removing the nonlinear terms in the vector fields) is found to be 3.1623 rad/s; whereas, for the 3-dof system the natural frequencies are 7.7084, 21.5983 and 31.2105 rad/s The harmonic support displacement for the sdof systems is given by $x_g(t) = x_{g0}\sin(\lambda t)$ with parameters $x_{g0} = 0.05\,\mathrm{m}$ and $\lambda = 4\,\mathrm{rad/s}$. It may be noted that the driving frequency is close to the natural frequency of the corresponding linear models in all the cases. The earthquake support motion considered for the 3-dof system is the El Centro (1940) ground acceleration. First 10 s of the earthquake acceleration, which contains the strong motion part, is considered for the simulation. In the simulations of the sdof systems, the measurements on velocity are assumed to be made. For the 3-dof system, on the other hand, the velocity of the third mass point is assumed to be measured. In the present study, all these measurements are synthetically (numerically) generated. While a uniform time step $h = 0.01$ s is used for simulating the Duffing and the 3-dof oscillators, the step size is halved to $h = 0.005$ s for the VDP oscillator. The ensemble sizes used are: $N = 100$ for the two sdof oscillators and $N = 200$ for the 3-dof system. To study the effect of initial conditions on the performance of the control system, the Duffing oscillator is simulated with three different initial conditions, with the initial condition vector $[x_0; \dot{x}_0]$ taking values [0.1; 0], [0.1; 0.5] and [0; 1], where x_0 is in m and $\dot{x}_0$ in m/s.

The SDRE control design requires expressing the equations of motion in the SDC form: $\dot{x} = A(x)x + B(x)u$. In all the examples considered here, $B(x)$ is a constant matrix. Thus the matrices $A(x)$ and $B(x)$ for the Duffing oscillator may be shown to be

$$A(x) = \begin{bmatrix} 0 & 1 \\ -\dfrac{\alpha + \beta x_1^2}{m} & -\dfrac{c}{m} \end{bmatrix} \quad \text{and} \quad B = \begin{Bmatrix} 0 \\ \dfrac{1}{m} \end{Bmatrix}. \tag{36}$$

Similarly, when the equation of motion for the VDP oscillator is expressed in the SDC form, the system matrices are given by

$$A(x) = \begin{bmatrix} 0 & 1 \\ -\dfrac{\alpha}{m} & -\dfrac{\mu(1 - x_1^2)}{m} \end{bmatrix} \quad \text{and} \quad B = \begin{Bmatrix} 0 \\ \dfrac{1}{m} \end{Bmatrix}. \tag{37}$$

For the 3-dof spring–mass system with bilinear springs, the SDC form of the equation of motion is obtained in a simple way. One readily observes that, for a system with linear springs having stiffness k_1, k_2 and k_3 (i.e. $\alpha_1 = k_1$, $\alpha_2 = k_2$, $\alpha_3 = k_3$, $\beta_1 = 0$, $\beta_2 = 0$ and $\beta_3 = 0$), the system matrix $A(x)$ is constant and is given by

$$A = \begin{bmatrix} 0_{3\times 3} & I_3 \\ -M^{-1}K & -M^{-1}C \end{bmatrix}, \tag{38}$$

where

$$M = \begin{bmatrix} m_1 & 0 & 0 \\ 0 & m_2 & 0 \\ 0 & 0 & m_3 \end{bmatrix}, \quad C = \begin{bmatrix} c_1 + c_2 & -c_2 & 0 \\ -c_2 & c_2 + c_3 & -c_3 \\ 0 & -c_3 & c_3 \end{bmatrix} \quad \text{and} \quad K = \begin{bmatrix} k_1 + k_2 & -k_2 & 0 \\ -k_2 & k_2 + k_3 & -k_3 \\ 0 & -k_3 & k_3 \end{bmatrix}. \tag{39}$$

$0_{3\times 3}$ is a 3×3 zero matrix and I_3 is a 3×3 identity matrix. However for the given system with bilinear springs, K is a state-dependent matrix $K_{\mathrm{eff}}(x)$ with elements k_1, k_2 and k_3 replaced by the effective stiffness coefficients $k_{\mathrm{eff},\,1}$, $k_{\mathrm{eff},\,2}$ and $k_{\mathrm{eff},\,3}$. Referring to Fig. 3(b), $k_{\mathrm{eff},\,i}$ $(i = 1, 2 \text{ and } 3)$, are computed as

$$k_{\mathrm{eff},i} = \begin{cases} \alpha_i & \text{if } |e_{x,i}| \leqslant x_{y,i}, \\ \dfrac{\alpha_i x_{y,i} + \beta_i(|e_{x,i}| - x_{y,i})}{|e_{x,i}|} & \text{otherwise.} \end{cases} \tag{40}$$

In Eq. (40), $e_{x,\,i}$ represents the extension of the ith spring. The system matrix $A(x)$in the SDC form is now obtained by replacing K with $K_{\text{eff}}(x)$ in Eq. (38). In the present work, two control configurations have been studied for the 3-dof structure. In case 1, the control force is applied at the third dof only; and in case 2, control forces are applied at all the three dofs. For the first case, the system matrix B is given by $B = \begin{bmatrix} 0 & 0 & 0 & 0 & 0 & 1/m_3 \end{bmatrix}^{\mathrm{T}}$ and, for the second case, it takes the form $B = \begin{bmatrix} 0_{3\times 3} & M^{-1} \end{bmatrix}^{\mathrm{T}}$. The weighing parameter $Q(x)$ is assumed to be of the form:

$$Q(x) = \begin{bmatrix} K(x) & 0 \\ 0 & 0 \end{bmatrix}. \tag{41}$$

$K(x)$ for the Duffing and VDP oscillators are chosen as $\alpha + \beta x_1^2$ and α respectively. For the 3-dof system, $K(x)$ is taken as $K_{\text{eff}}(x)$. 0 in Eq. (41) represents a zero matrix having the same size as $K(x)$. The weighing parameter $R(x)$ is assumed to be constant, whose values for the Duffing and VDP oscillators are taken as 0.001 and 1, respectively. For the 3-dof system its value is taken as 0.001 for case 1 and $0.001I_3$ for case 2. It may be noted here that the weighing parameters $Q(x)$ and $R(x)$ are design parameter functions that are chosen to provide the desired response. Thus, one can tune these parameters for reshaping the response. The choice of $Q(x)$ as in Eq. (41) makes the first term of the cost function (Eq. (8)) to represent the structural strain energy. The parameter $R(x)$ determines the relative importance of control effectiveness and economy; for instance, a smaller value implies greater weight on control effectiveness. In any given situation, one needs to take into account the limits on available control resources before a meaningful value of $R(x)$ could be selected. A suite of digital simulations would further provide essential insights into levels to which the response could in turn be controlled. In the present study, it was found that the proposed algorithms performed satisfactorily for a wide choice of $R(x)$ and in the present paper we provide a subset of results from this investigation.

In the simulations of all the example problems considered here, we mainly use the bootstrap filter for state estimation. However, given the limitations of the bootstrap filter, its performance in state estimation has been compared with that of the SIS filter in all the cases. In implementing the SIS filter, the threshold of the effective sample size (that decides the need for resampling) is taken to be 1/3rd of the sample size. It may be noted that the control responses shown in the figures are those obtained by control algorithms employing bootstrap filter, unless otherwise mentioned explicitly. The estimated velocity history and the associated variance histories of the estimators for displacement and velocity are shown in Fig. 4. Fig. 4(a) also plots the measurement taken on the velocity. Fig. 4(b) shows a comparison of the variance of the states estimated by the control algorithm with bootstrap filter and SIS-based filter. As anticipated, a significant reduction in the variance can be observed when the algorithm uses the SIS filter. Fig. 5 shows a comparison of the uncontrolled and controlled responses of the Duffing oscillator in the 1-period regime. Apart from a drastic reduction of the response amplitude, the type of dynamical response also changes from a dumb-bell shaped to an elliptical orbit with the application of the control force. Fig. 6 shows six different realizations of the velocity history of the Duffing oscillator under two different schemes of measurements—(i) displacement alone is measured and (ii) velocity alone is measured. The results obtained when bootstrap filter and SIS filter are used for state estimation, are given separately. One can observe the robustness of the algorithm with both the filters under both schemes of measurement. Fig. 7 shows the phase plane plots of the Duffing oscillator, for uncontrolled and controlled cases, for different initial conditions. One may easily see that irrespective of the initial conditions, the control force drives the system close to the origin, which is a stable equilibrium point. Simulation results of the VDP oscillator are reported in Figs. 8 and 9. Again, the effectiveness of the estimation as well as the control algorithm is clearly brought out. This is probably also indicative of the applicability of the proposed schemes for different types of nonlinearities in the vector field. One may also observe from Fig. 9(b) that the origin, which is an unstable fixed point in the uncontrolled case, becomes stable owing to a possible modification of the system parameters by the control force and, the control force drives the system to the origin.

Figs. 10–14 show the results on simulations of the 3-dof oscillator. Fig. 10 shows a comparison of the variance associated with state estimation using bootstrap and SIS filters for control case 2. Similar results are obtained for case 1 also. Here also, one can observe the superiority of the SIS filter over bootstrap filter. Comparisons of the time histories of the relative displacement of the third mass point for the uncontrolled and controlled systems (corresponding to cases 1 and 2) are shown in Fig. 11. A similar comparison of the phase

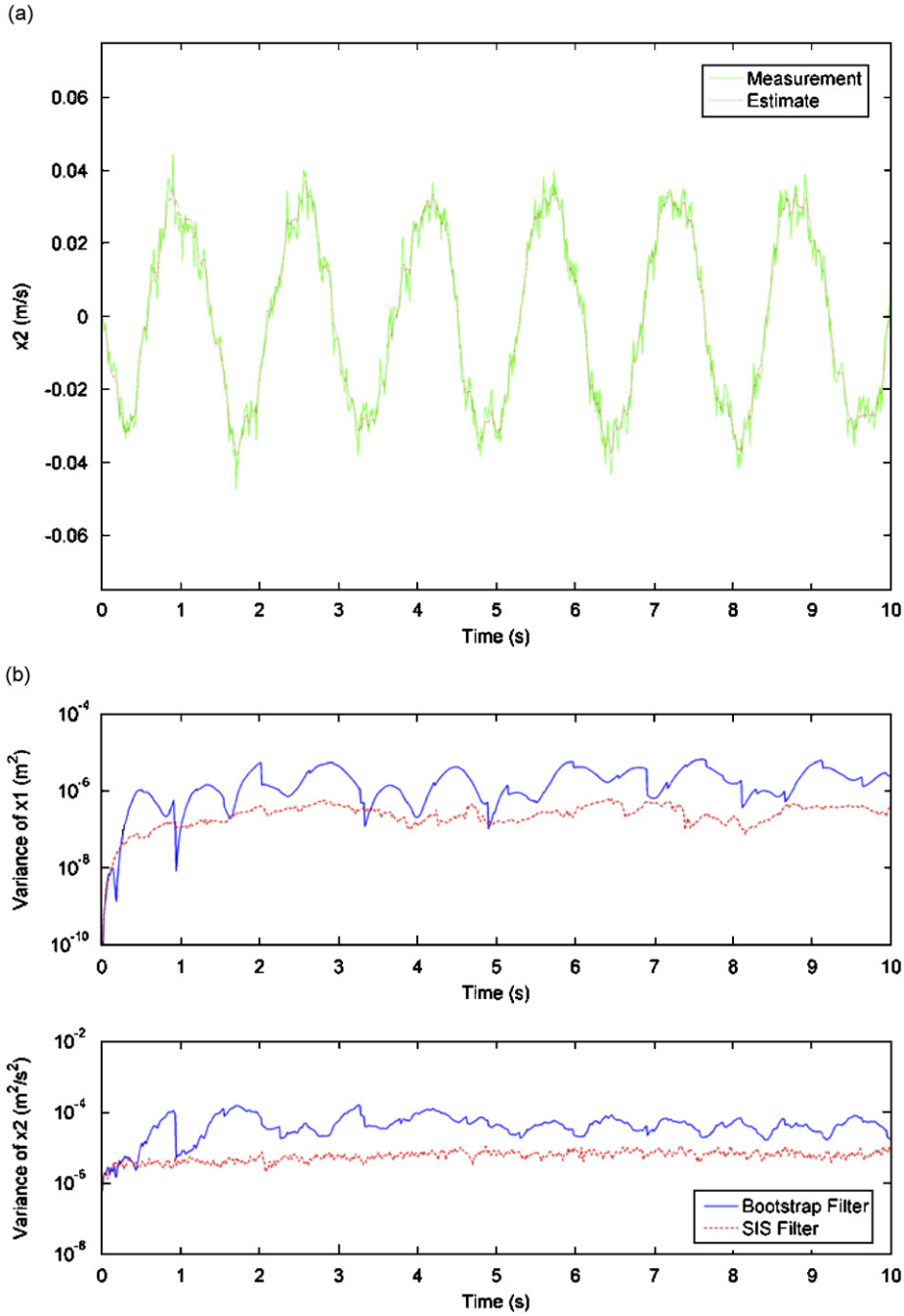

Fig. 4. State estimation of the Duffing oscillator: (a) measured and estimated velocity (x_2) and (b) performance of bootstrap filter and SIS filter in state estimation.

plane plots of the states is shown in Fig. 12. That case 2 performs better as a control strategy than case 1 should be clear from these figures. The control configuration in case 2 obviously corresponds to the smallest reaction force and this is indicated in Fig. 13, which shows the time histories of the force in the first spring, for different cases. The force-displacement graphs for all springs, for various control cases, are compared in Fig. 14. As can be seen from this figure, the displacement of the uncontrolled system is excessive and all the springs cross the critical point; and, in the controlled system, the springs remain within the linear range by and

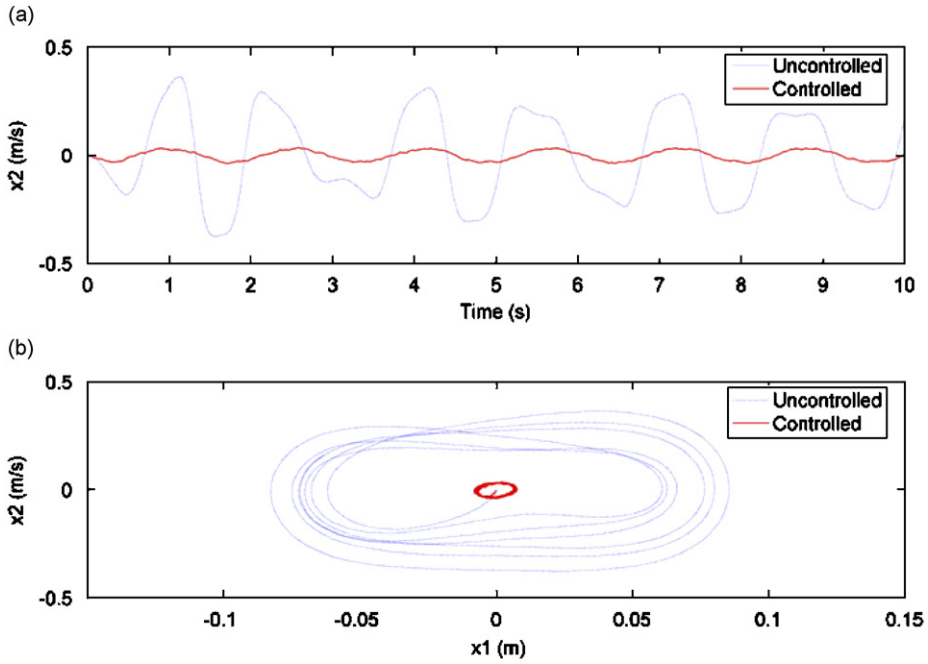

Fig. 5. Uncontrolled and controlled response of Duffing oscillator: (a) time history of velocity and (b) phase plane plot.

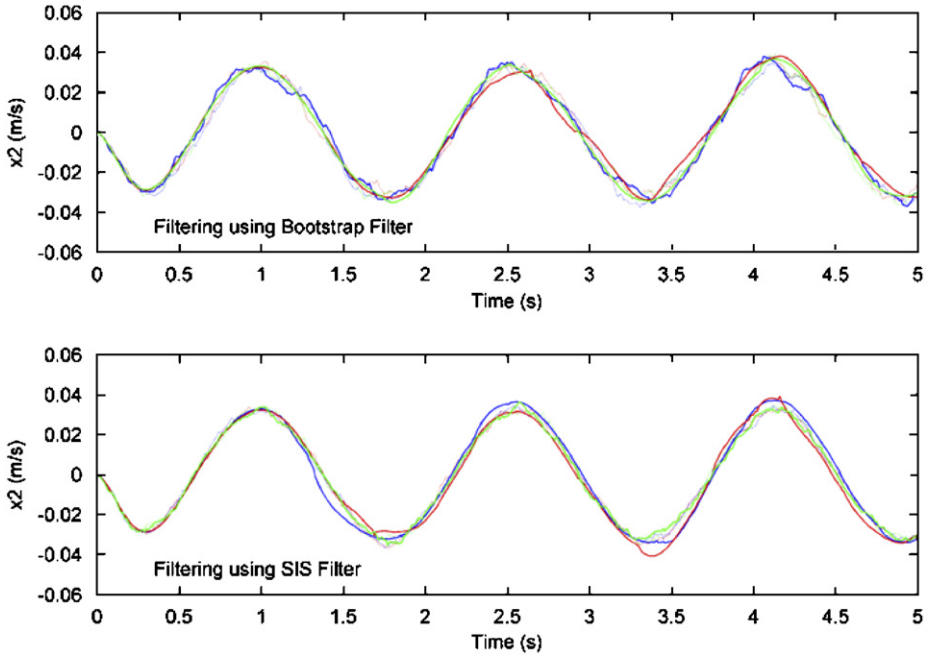

Fig. 6. Six different realizations of the time history of velocity of the Duffing oscillator, with states estimated using bootstrap filter and SIS filter under two different measurement schemes: (i) displacement alone is measured (time history with solid lines) and (ii) velocity alone is measured (time history with dotted lines).

large. It may be noted here that the superiority in the performance of the SIS filter compared to that of the bootstrap filter in control algorithms is at the expense of the increased computational cost. It has been observed that the simulation time for the SIS filter-based control system is approximately 50% more

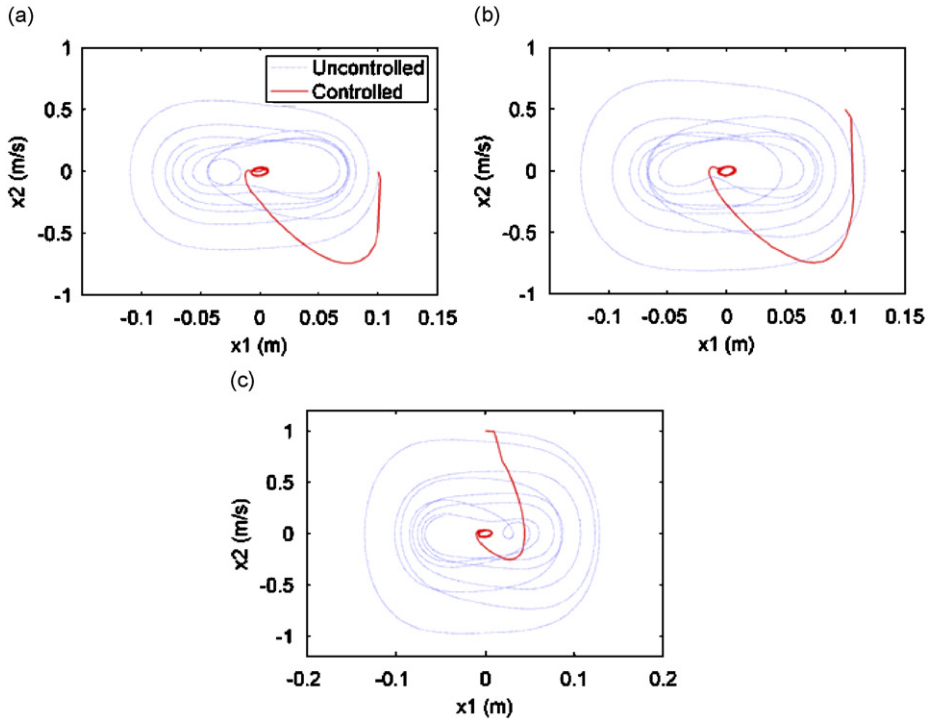

Fig. 7. Phase plane plots of the Duffing oscillator for different initial conditions: (a) $x_0 = 0.1\,\mathrm{m}$, $\dot{x}_0 = 0\,\mathrm{m/s}$, (b) $x_0 = 0.1\,\mathrm{m}$, $\dot{x}_0 = 0.5\,\mathrm{m/s}$ and (c) $x_0 = 0\,\mathrm{m}$, $\dot{x}_0 = 1\,\mathrm{m/s}$.

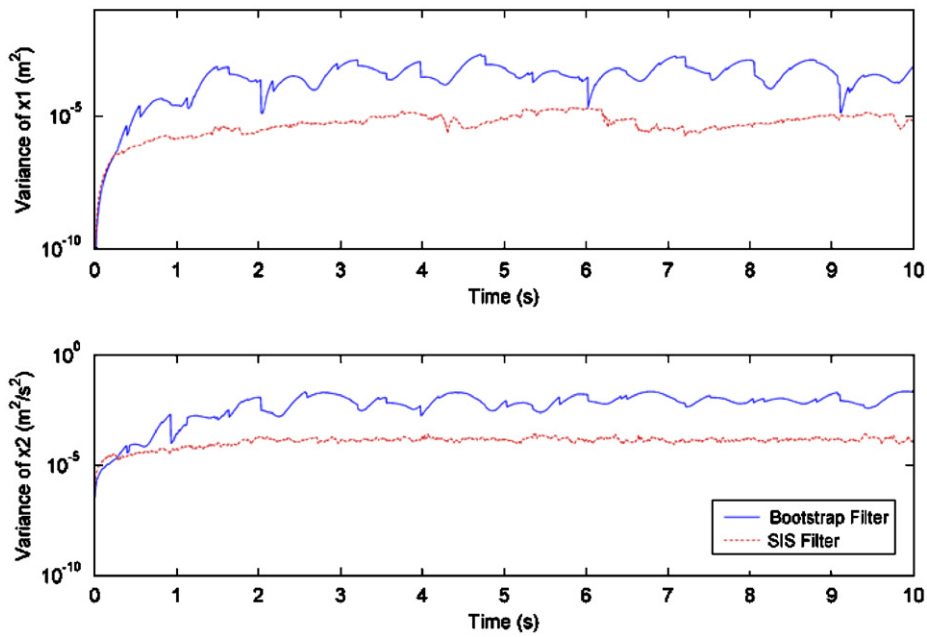

Fig. 8. Performance of bootstrap filter and SIS filter in state estimation of the VDP oscillator.

compared to that of the system employing bootstrap filter, for sdof oscillators; and, for the 3-dof system it is 115% more. This increase in time is attributable to the extra computational effort needed for drawing samples from the (multidimensional) importance density function.

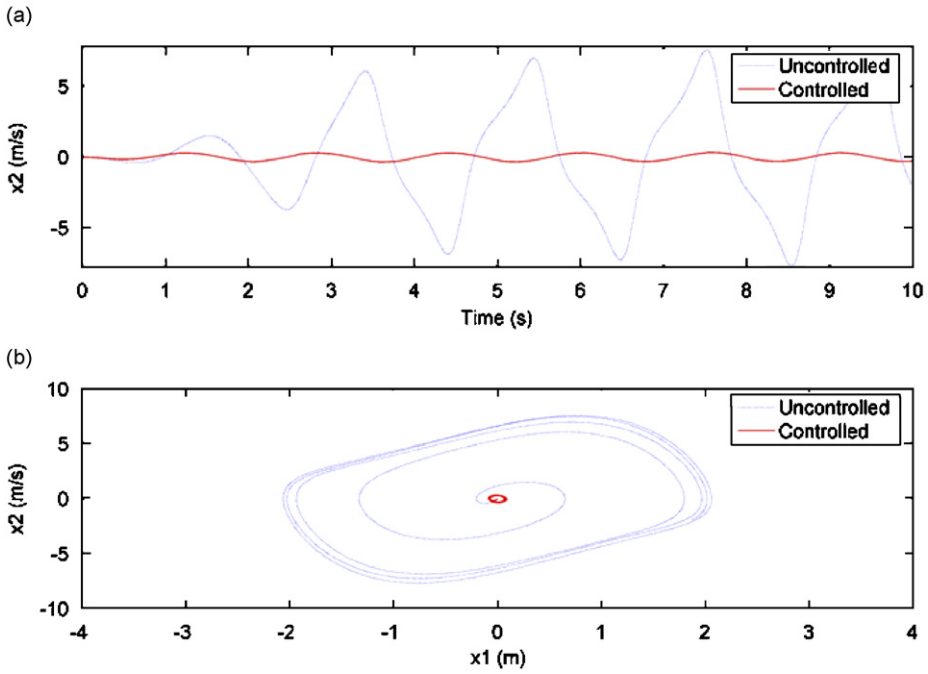

Fig. 9. Uncontrolled and controlled response of VDP oscillator: (a) time history of displacement and (b) phase plane plot.

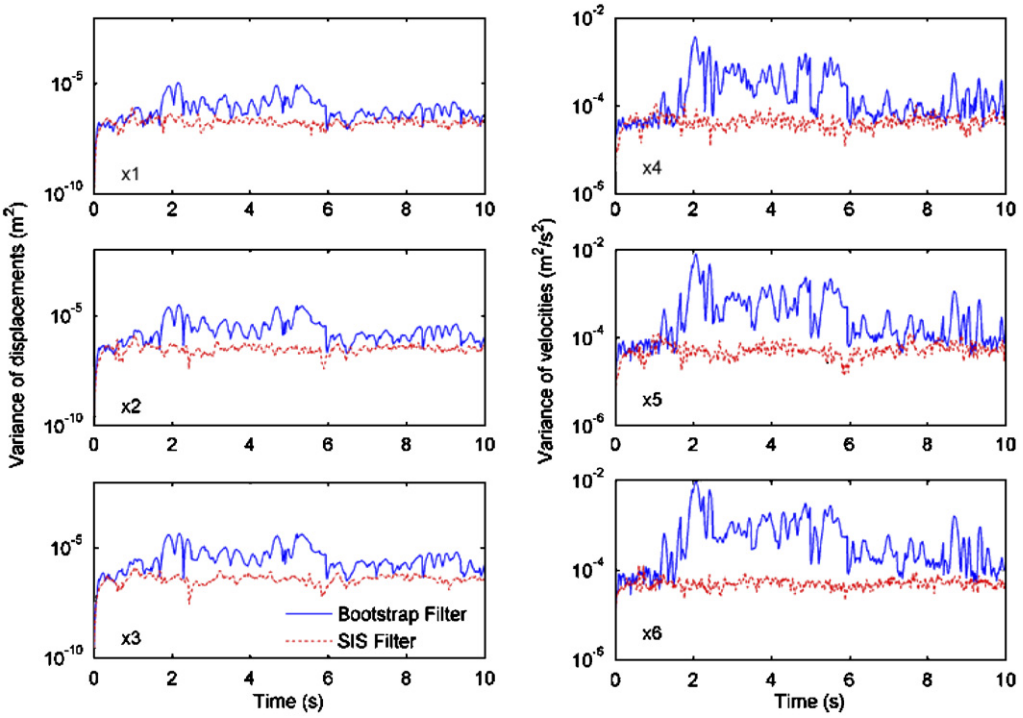

Fig. 10. Comparison of the performance of the bootstrap and SIS filters in state estimation of the 3-dof oscillator (case 2).

All the simulation results (except Fig. 6) shown here are in the form of single specific realizations of the response. In order to assess the overall performance of the proposed algorithm with respect to sampling fluctuations, for a given realization of the measurement noise, 100 Monte Carlo simulations, each with a

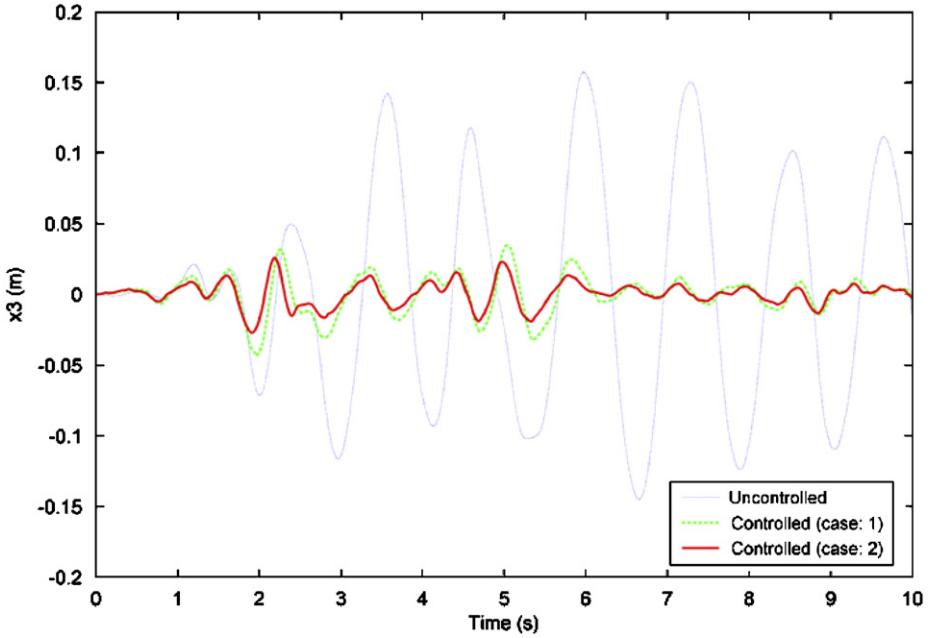

Fig. 11. Comparison of the relative displacement of the third mass point of the 3-dof system for uncontrolled and controlled cases.

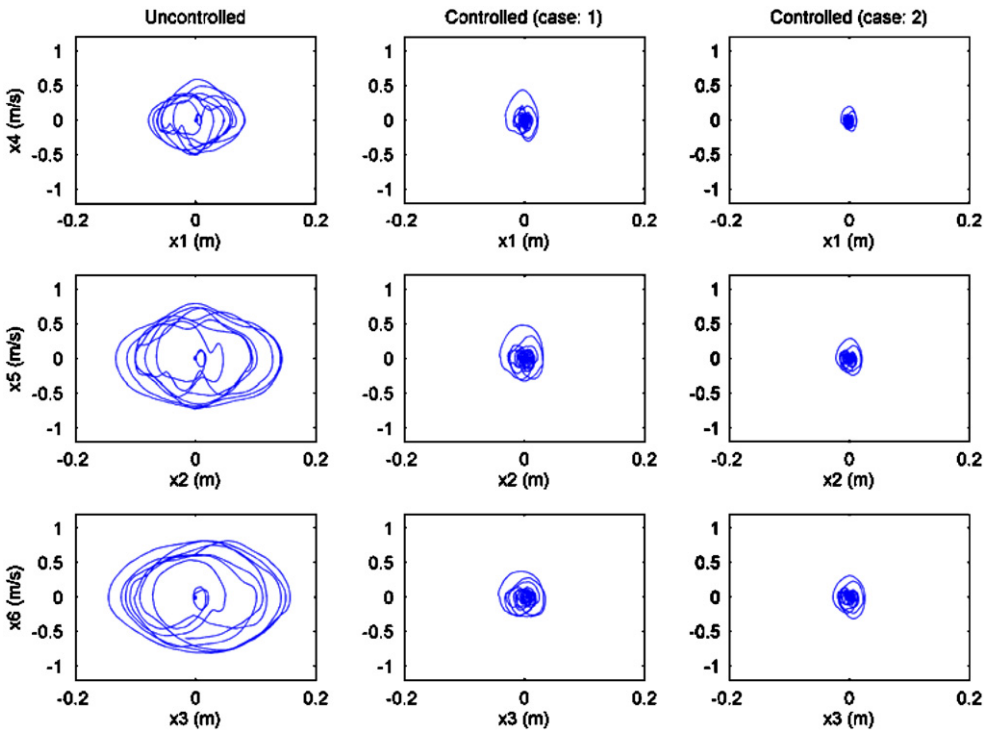

Fig. 12. Comparison of the phase plane plots of the 3-dof system for uncontrolled and controlled cases.

sample size of 200, are performed on the 3-dof system and the time history of the displacement of the third mass point in five different runs is shown in Fig. 15. The robustness of the algorithm may be observed for both control cases. Also, the average values of the peak response quantities, peak control forces and control

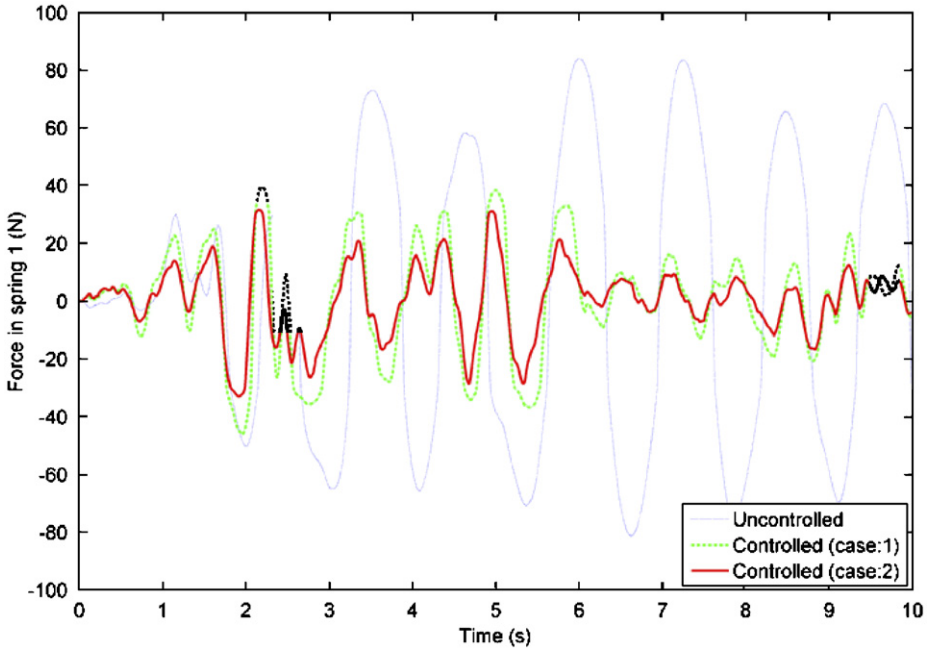

Fig. 13. Comparison of the time history of the force in the first spring of the 3-dof system for uncontrolled and controlled cases.

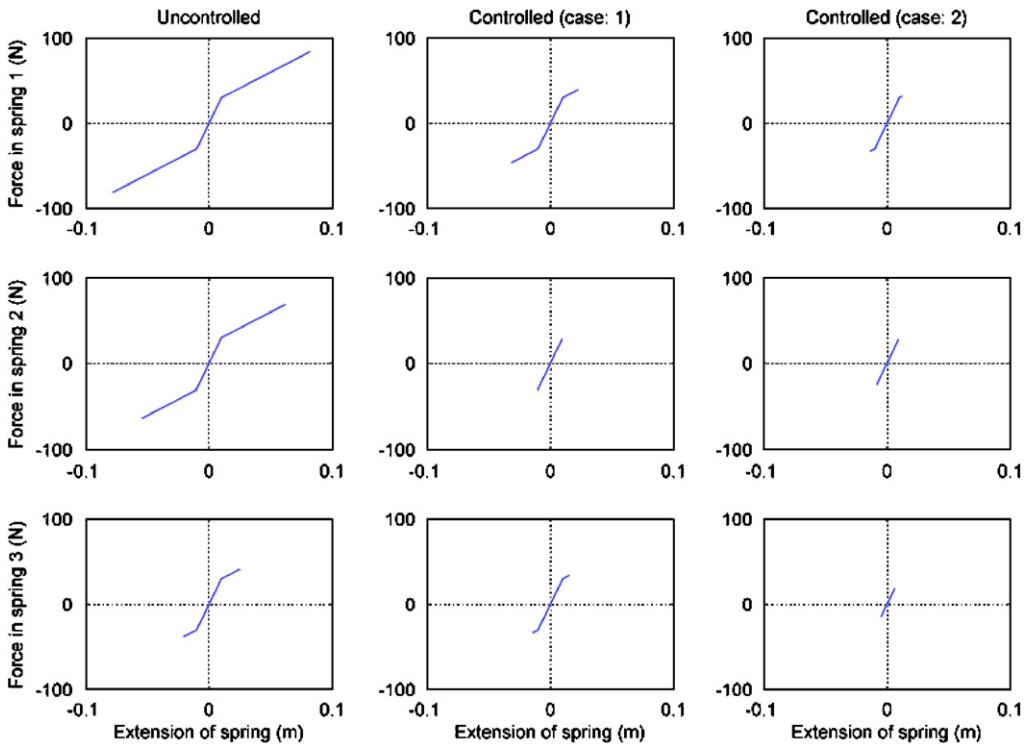

Fig. 14. Comparison of the force-displacement graphs for various springs of the 3-dof system for uncontrolled and controlled cases.

efficiencies are tabulated in Table 1. The control efficiency is calculated as $100(\|x_{uc}\|_{max}-\|x_c\|_{max})/\|x_{uc}\|_{max}$, where $\|\cdot\|$ represents the Euclidian norm, x_{uc} and x_c represent the state vectors in the uncontrolled and controlled cases, respectively. A higher efficiency in control case 2 is observable compared to case 1. It is again

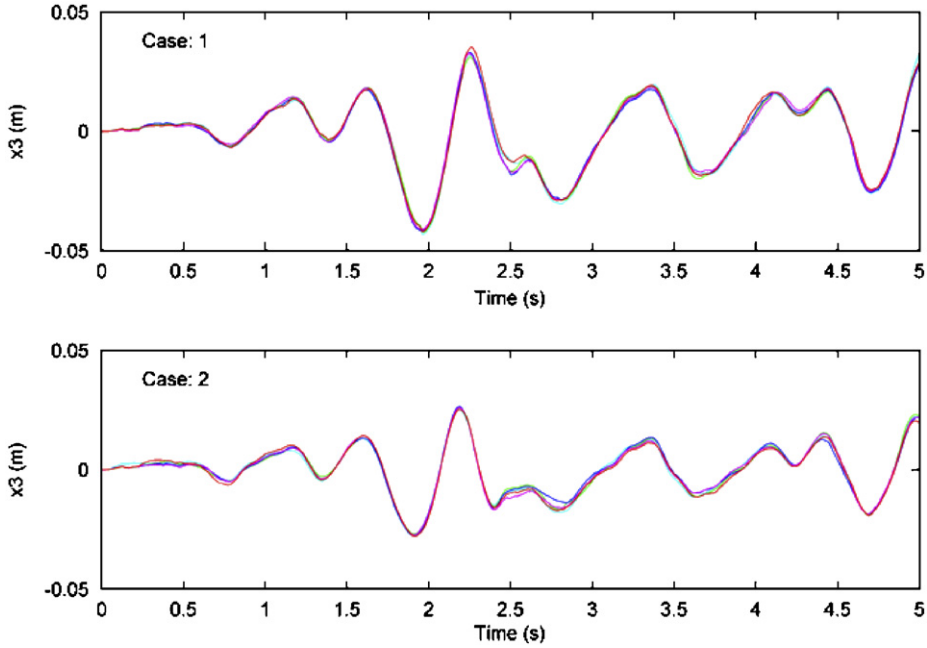

Fig. 15. Five different realizations of the time history of the displacement of the third mass point, of the 3-dof system, for control cases 1 and 2.

emphasized that, depending on the available control resources, one may tune the control parameters in order to obtain a desirable level of control. To assess the performance of the algorithm for different particle sizes, for a given realization of the measurement noise, 100 Monte Carlo simulations are performed on the 3-dof system, under control case 1, with $N = 50$, 100, 200, 1000 and 3000. The mean values of the estimated states of the system corresponding to a given time instant (taken as $t = 2.5$ s.) for different sample sizes are shown in Fig. 16. The 95% probability bounds are also marked. It may be readily observed that the dispersion from the mean, which is a consequence of the sampling fluctuations, reduces consistently with increase in particle size.

7. Concluding remarks

The problem of active control of nonlinear oscillators, especially those of interest in structural engineering, is considered while incorporating both process and measurement noises. The Monte Carlo filters, popularly known as particle filters, are identified as powerful tools for estimation of the controlled states of such nonlinear systems. Particle filters are observed to be very useful in feedback control applications of nonlinear structural dynamical systems, which require the estimation of full states of the systems from a few noisy measurements available. Despite its versatility, the particle filter has not been made use of for control of nonlinear structures with noise. To the best of authors' knowledge, the present work constitutes the first attempt at demonstrating the usefulness of particle filters in control of nonlinear structural dynamical systems. Presently, both the Bayesian boot strap filter and that based on sequential importance sampling have been used for state estimation. The SIS filter provides more accurate estimation at the expense of increased computational time. Indeed, in the context of real-time control applications, the bootstrap filter offers a simple and reasonably accurate state estimation tool. However, as more advanced particle filters are available and new schemes of variance reductions (variance due to finiteness of ensemble sizes) come into existence, the issue of relative suitability of different types of particle filters in control applications would pose an interesting problem. A more detailed exploration of this issue is however beyond the scope of this study. The particle filters require discrete maps to work with, and, hence, the continuous forms of the SDEs, representing the

Table 1
Average values of peak response, peak control force and control efficiency of the 3-dof system, over 100 Monte Carlo simulations

		Max. values of displacements & velocities						Max. force in springs (N)			Max. control force (N)			Control efficiency (%)
		x_{1max} (m)	x_{2max} (m)	x_{3max} (m)	x_{4max} (m/s)	x_{5max} (m/s)	x_{6max} (m/s)	1	2	3	u_{1max}	u_{2max}	u_{3max}	
	Uncontrolled	0.0938 (0.0089)	0.1587 (0.0124)	0.1772 (0.0180)	0.5786 (0.0349)	0.8576 (0.0724)	0.9198 (0.0888)	92.88 (6.78)	72.75 (3.55)	41.60 (2.68)	–	–	–	–
Case 1	Controlled	0.0233 (0.0007)	0.0316 (0.0009)	0.0330 (0.0016)	0.4036 (0.0102)	0.4730 (0.0111)	0.3658 (0.0069)	40.01 (0.55)	28.51 (1.02)	34.05 (0.50)	–	–	37.03 (0.58)	45.2
	% Reduction	75.2	80.1	81.4	30.24	44.84	60.23	56.9	60.8	18.1	–	–	–	
Case 2	Controlled	0.0122 (0.0005)	0.0210 (0.0008)	0.0259 (0.001)	0.1994 (0.0089)	0.2941 (0.0069)	0.3203 (0.0056)	31.63 (0. 40)	26.42 (0.71)	18.69 (0.54)	18.08 (0.58)	26.65 (0.69)	28.66 (0.73)	64.0
	% Reduction	87.0	86.8	85.4	65.5	65.7	61.2	65.9	63.7	55.1				

Note: Values written in parenthesis represent the associated standard deviation.

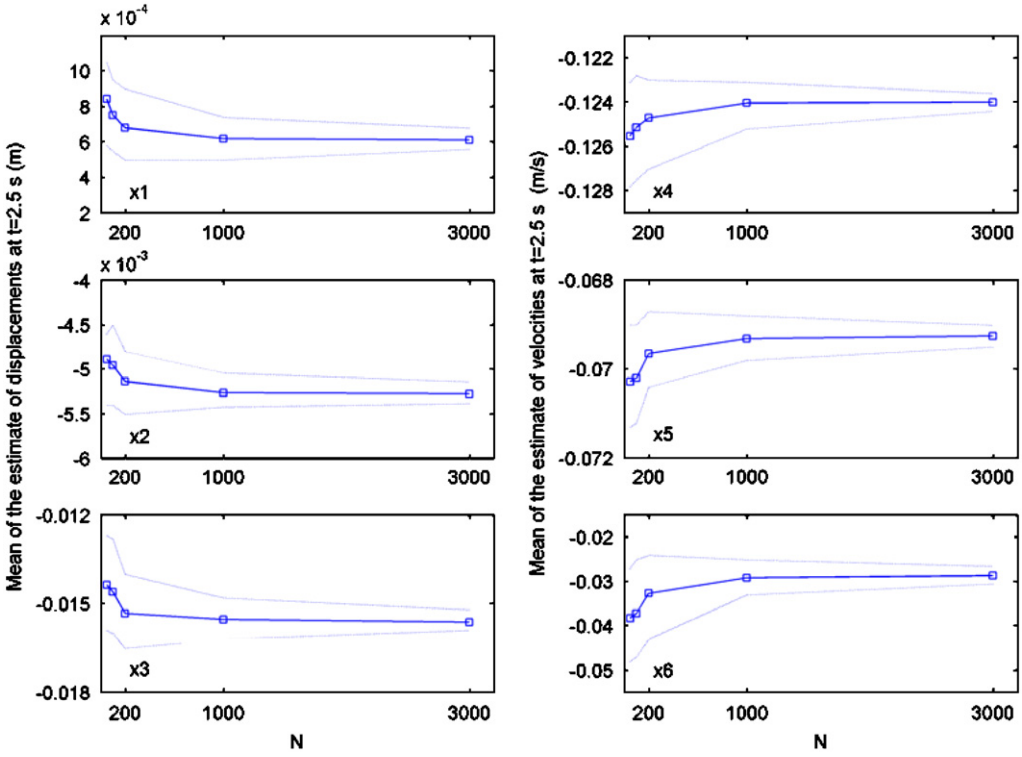

Fig. 16. The mean, over 100 Monte Carlo simulations, of the estimate of the displacement and velocity components of the 3-dof system at $t = 2.5$ s. for control case 1, for different particle sizes (solid lines show the mean and dotted lines show the 95% probability bounds).

process equations, are discretized using an explicit form of the Ito–Taylor expansion. This exercise leads to discrete maps of displacements and velocities to a high formal order of accuracy provided that the vector field is adequately differentiable. The control design is done by the SDRE method, which has gained considerable attention in recent years among the researchers working in control of nonlinear systems. To demonstrate the effectiveness of particle filters in control of nonlinear structures, we have considered two sdof systems, viz., the Duffing and VDP oscillators and, a 3-dof nonlinear oscillator with bilinear springs. Based on the simulations, the performance of particle filters in control of nonlinear structures is observed to be excellent. Also, the SDRE method is found to be very attractive for designing control laws for nonlinear structural systems.

Only a numerical route is presently chosen to demonstrate the use of particle filters in structural control applications. However, with high speed processors and suitable actuating devices, the proposed strategy can potentially be used for practical implementations. To account for inherent time delays of actuators, one can use a suitable extrapolation strategy to predict the actuator displacement so that it can be commanded in advance to generate the required control force accurately. It must be understood that real-time control applications of nonlinear structures, especially those with large dimensions, require that the computations proceed as fast as possible. Though different versions of EKFs, which could handle nonlinearity, are available, particle filters are far more versatile in their ability to handle system nonlinearity and can even account for the non-Gaussian nature of the response and noise processes. However, given that Monte Carlo simulations, based on numerical integrations of mathematical models of structures, are computationally too demanding, alternative semi-analytical routes (such as the ones based on linearizations of the governing SDEs) must be explored for speeding up the simulations. In this context, the issue of variance reduction of the estimated states also assumes importance as this may potentially reduce the ensemble size drastically. Investigations on these lines constitute interesting elements of future research.

Appendix. The stochastic Taylor expansion

Consider the vector stochastic process $x(t) := \{x^{(i)}(t) | i \in [1,n]\} \in \Re^n$ governed by the system of SDEs:

$$\mathrm{d}x(t) = a(t,x)\,\mathrm{d}t + \sum_{r=1}^{q} \sigma_r(t,x)\,\mathrm{d}B_r(t), \tag{A.1}$$

where $B(t) := \{B_r(t)\} \in \Re^q$ is a q dimensional vector Wiener (Brownian motion) process, $a(t,x) := \{a^{(i)}(t,x) | i \in [1,n]\} : \Re \times \Re^n \to \Re^n$ is the drift vector and $\sigma_r(t,x) : \Re \times \Re^n \to \Re^n$ is the rth column of the diffusion matrix $[\sigma]_{n\times q}$. Let $f(t,x) : \Re \times \Re^n \to \Re$ be a sufficiently smooth scalar function. Then, by Ito's formula [56], one can write

$$\mathrm{d}f(t,x) = \frac{\partial}{\partial t} f(t,x)\,\mathrm{d}t + \sum_{i=1}^{n} \frac{\partial}{\partial x^{(i)}} f(t,x)\,\mathrm{d}x^{(i)} + \frac{1}{2}\sum_{i,j=1}^{n} \frac{\partial^2}{\partial x^{(i)}\partial x^{(j)}} f(t,x)\,\mathrm{d}x^{(i)}\,\mathrm{d}x^{(j)}. \tag{A.2}$$

Note that $\mathrm{d}x^{(i)}\,\mathrm{d}x^{(j)}$ needs be calculated according to the rule: $\mathrm{d}t\,\mathrm{d}t = \mathrm{d}t\,\mathrm{d}B_r = \mathrm{d}B_r\,\mathrm{d}t = 0$ and $\mathrm{d}B_r\,\mathrm{d}B_r = \mathrm{d}t$. Now, from Eq. (A.2), one can write for $t_0 \leqslant t \leqslant s$:

$$f(s,x(s)) = f(t,x) + \sum_{r=1}^{q} \int_t^s \Lambda_r f(s_1, x(s_1))\,\mathrm{d}B_r(s_1) + \int_t^s Lf(s_1, x(s_1))\,\mathrm{d}s_1, \tag{A.3}$$

where the operators Λ_r and L are, respectively, given by

$$\Lambda_r = \sum_{j=1}^{n} \sigma_r^{(j)} \frac{\partial}{\partial x^{(j)}}, \tag{A.4a}$$

$$L = \frac{\partial}{\partial t} + \sum_{j=1}^{n} a^{(j)}(t,x)\frac{\partial}{\partial x^{(j)}} + \frac{1}{2}\sum_{r=1}^{q}\sum_{i,j=1}^{n} \sigma_r^{(i)}\sigma_r^{(j)} \frac{\partial^2}{\partial x^{(i)}\partial x^{(j)}}. \tag{A.4b}$$

Now, applying Eq. (A.3) repeatedly to $f(s_1, x(s_1))$ one gets

$$\begin{aligned} f(t+h, x(t+h)) = f(t,x) &+ \sum_{r=1}^{q} \Lambda_r f \int_t^{t+h} \mathrm{d}B_r(s) + Lf \int_t^{t+h} \mathrm{d}s \\ &+ \sum_{r=1}^{q}\sum_{i=1}^{q} \Lambda_i\Lambda_r f \int_t^{t+h}\int_t^s \mathrm{d}B_r(s_1)\,\mathrm{d}B_i(s) \\ &+ \sum_{r=1}^{q}\sum_{i,j=1}^{q} \Lambda_j\Lambda_i\Lambda_r f \int_t^{t+h}\int_t^s\int_t^{s_1} \mathrm{d}B_j(s_2)\,\mathrm{d}B_i(s_1)\,\mathrm{d}B_r(s) \\ &+ \sum_{r=1}^{q} \Lambda_r Lf \int_t^{t+h}\int_t^s \mathrm{d}B_r(s_1)\,\mathrm{d}s + \sum_{r=1}^{q} L\Lambda_r f \int_t^{t+h}\int_t^s \mathrm{d}s_1\,\mathrm{d}B_r(s) \\ &+ \sum_{r=1}^{q}\sum_{i=1}^{q} L\Lambda_i\Lambda_r f \int_t^{t+h}\int_t^s\int_t^{s_1} \mathrm{d}B_i(s_2)\,\mathrm{d}B_r(s_1)\,\mathrm{d}s \\ &+ \sum_{r=1}^{q}\sum_{i=1}^{q} \Lambda_i L\Lambda_r f \int_t^{t+h}\int_t^s\int_t^{s_1} \mathrm{d}B_i(s_2)\,\mathrm{d}s_1\,\mathrm{d}B_r(s) \\ &+ L^2 f \int_t^{t+h}\int_t^s \mathrm{d}s_1\,\mathrm{d}s + \rho, \end{aligned} \tag{A.5}$$

where ρ is the set of remainder terms. One can still expand the remainder terms using Eq. (A.3) to get higher order terms in the expansion. The integrals, in this expression, involving increments of Wiener components $\mathrm{d}B_r(t)$ are referred to as multiple stochastic integrals (MSIs).

References

[1] J.T.P. Yao, Concept of structural control, *Journal of Structural Engineering ASCE* 98 (1972) 1567–1574.
[2] T.T. Soong, *Active Structural Control: Theory and Practice*, Longman Scientific and Technical, New York, 1990.
[3] G.W. Housner, L.A. Bergman, T.K. Caughey, A.G. Chassiakos, R.O. Claus, S.F. Masri, R.E. Skelton, T.T. Soong, B.F. Spencer, J.T.P. Yao, Structural control: past, present and future, *Journal of Engineering Mechanics* 123 (1997) 897–971.
[4] T.K. Datta, A state-of-the-art review on active control of structures, *ISET Journal of Earthquake Technology* 40 (2003) 1–17.
[5] H.J. Marquez, *Nonlinear Control Systems—Analysis and Design*, Wiley, New York, 2003.
[6] H.K. Khalil, *Nonlinear Systems*, Prentice-Hall Inc., Englewood Cliffs, NJ, 2002.
[7] J.R. Cloutier, State-dependent Riccati equation techniques: an overview, *Proceedings of the American Control Conference*, 1997, pp. 932–936.
[8] J.R. Cloutier, D.T. Stansbery, The capabilities and art of state-dependant Riccati equation based design, *Proceedings of the American Control Conference*, 2002, pp. 86–91.
[9] J.S. Shamma, J.R. Cloutier, Existence of SDRE stabilizing feedback, *Proceedings of the American Control Conference*, 2001, pp. 4253–4257.
[10] E.B. Erdem, A.G. Alleyne, Globally stabilizing second order nonlinear systems by SDRE control, *Proceedings of the American Control Conference*, 1999, pp. 2501–2505.
[11] W. Langson, A.G. Alleyne, A stability result with application to nonlinear regulation: theory and experiments, *Proceedings of the American Control Conference*, 1999, pp. 3051–3056.
[12] K.D. Hammett, D.B. Ridgely, Locally stabilizing analytic state feedback controllers for scalar systems via SDRE nonlinear regulation, *Proceedings of the American Control Conference*, 1997, pp. 1070–1071.
[13] J.W. Curtis, R.W. Beard, Ensuring stability of state-dependent Riccati equation controllers via satisficing, *Proceedings of the American Control Conference*, 2002, pp. 2645–2650.
[14] M. Innocenti, F. Baralli, F. Salotti, A. Caiti, Manipulator path control using SDRE, *Proceedings of the American Control Conference*, 2000, pp. 3348–3352.
[15] P.K. Menon, T. Lam, L.S. Crawford, V.H.L Cheng, Real-time computational methods of SDRE nonlinear control of missiles, *Proceedings of the American Control Conference*, 2002, pp. 232–237.
[16] K.A. Wise, J.L. Sedwick, Nonlinear control of agile missiles using state dependent Riccati equations, *Proceedings of the American Control Conference*, 1997, pp. 379–380.
[17] D.K. Parrish, D.B. Ridgely, Attitude control of a satellite using SDRE method, *Proceedings of the American Control Conference*, 1997, pp. 942–945.
[18] E.A. Wan, A.A. Bogdanov, Model predictive neural control with applications to a 6 DOF helicopter model, *Proceedings of the American Control Conference*, 2001, pp. 488–493.
[19] S.N. Singh, W. Yim, State feedback control of an aeroelastic system with structural nonlinearity, *Aerospace Science and Technology* (2003) 23–31.
[20] W. Ren, R.W. Beard, Constrained nonlinear tracking control for small fixed-wing unmanned air vehicles, *Proceedings of the American Control Conference*, 2004, pp. 4663–4668.
[21] D.K. Parrish, D.B. Ridgely, Control of an artificial human pancreas using the SDRE method, *Proceedings of the American Control Conference*, 1997, pp. 1059–1060.
[22] S.F. Masri, G.A. Bekey, T.K. Caughey, On-line control of nonlinear flexible structures, *Journal of Applied Mechanics* 49 (1981) 871–884.
[23] A.M. Reinhorn, G.D. Manolis, C.Y. Wen, Active control of inelastic structures, *Journal of Engineering Mechanics* 113 (1987) 315–333.
[24] A.M. Rohman, A.H. Nayfeh, Active control of nonlinear oscillations in bridges, *Journal of Engineering Mechanics* 113 (1987) 335–348.
[25] A.H. Barbat, J. Rodellar, E.P. Ryan, N. Molinares, Active control of nonlinear base-isolated buildings, *Journal of Engineering Mechanics* 121 (1995) 676–684.
[26] J.N. Yang, J.C. Wu, A.K. Agrawal, Sliding mode control for nonlinear and hysteretic structures, *Journal of Engineering Mechanics* 121 (1995) 1330–1339.
[27] M. Tadi, Nonlinear feedback control of slewing beams, *Computer Methods in Applied Mechanics and Engineering* 195 (2006) 133–147.
[28] R. Ghanem, M. Bujakov, K. Torikoshi, H. Itoh, T. Inazuka, H. Hiei, T. Watanabe, Adaptive control of nonlinear uncertain dynamical systems, *Journal of Engineering Mechanics* 123 (1997) 1161–1169.
[29] J. Suhardio, B.F. Spencer Jr., M.K. Sain, Nonlinear optimal control of a Duffing system, *International Journal of Nonlinear Mechanics* 27 (1992) 157–172.
[30] J.N. Yang, A.K. Agrawal, S. Chen, Optimal polynomial control for seismically excited nonlinear and hysteretic structures, *Earthquake Engineering and Structural Dynamics* 25 (1996) 1211–1230.
[31] A.K. Agrawal, J.N. Yang, J.C. Wu, Nonlinear control strategies for Duffing systems, *International Journal of Nonlinear Mechanics* 33 (1998) 829–841.
[32] W.Q. Zhu, G. Ying, T.T. Soong, An optimal nonlinear feedback control strategy for randomly excited structural systems, *Nonlinear Dynamics* 24 (2001) 31–51.

[33] Z.G. Ying, W.Q. Zhu, T.T. Soong, A stochastic optimal semi-active control strategy for ER/MR dampers, *Journal of Sound and Vibration* 259 (2003) 45–62.
[34] W.Q. Zhu, Z.G. Ying, Y.Q. Ni, J.M. Ko, Optimal nonlinear stochastic control of hysteretic systems, *Journal of Engineering Mechanics* 126 (2000) 1027–1032.
[35] W.Q. Zhu, Nonlinear stochastic dynamics and control in Hamiltonian formulation, *Applied Mechanics Reviews* 59 (2006) 230–248.
[36] L.L. Chung, C.C. Lin, S.Y. Chu, Optimal direct output feedback of structural control, *Journal of Engineering Mechanics* 119 (1993) 2157–2173.
[37] R.F. Stengel, *Optimal Control and Estimation*, Dover Publications, Inc., New York, 1994.
[38] J.J. Beaman, Nonlinear quadratic Gaussian control, *International Journal of Control* 39 (1984) 343–361.
[39] A.N. Atassi, H.K. Khalil, A separation principle for the stabilization of a class of nonlinear systems, *IEEE Transactions on Automatic Control* 44 (1999) 1672–1687.
[40] A.N. Atassi, H.K. Khalil, A separation principle for the control of a class of nonlinear systems, *IEEE Transactions on Automatic Control* 46 (2001) 1672–1687.
[41] H.M. Park, W.J. Lee, Feedback control of natural convection, *Computer Methods in Applied Mechanics and Engineering* 191 (2001) 1013–1028.
[42] T. Schauer, N.O. Negard, F. Previdi, K.J. Hunt, M.H. Fraser, E. Ferchland, T. Raisch, Online identification and nonlinear control of the electrically stimulated quadriceps muscle, *Control Engineering Practice* 13 (2005) 1207–1219.
[43] R.E. Kalman, A new approach to linear filtering and prediction problems, *Transactions of the ASME – Journal of Basic Engineering* 82 (Series D) (1960) 35–45.
[44] R.G. Brown, P.Y.C. Hwang, *Introduction to Random Signals and Applied Kalman Filtering*, Wiley, New York, 1992.
[45] N.J. Gordon, D.J. Salmond, A.F.M. Smith, Novel approach to nonlinear/non-Gaussian Bayesian state estimation, *IEE Proceedings-F* 140 (1993) 107–113.
[46] H. Tanizaki, *Nonlinear Filters: Estimation and Applications*, Springer, Berlin, 1996.
[47] H. Tanizaki, R.S. Mariano, Nonlinear and non-Gaussian state-space modeling with Monte Carlo simulations, *Journal of Econometrics* 83 (1998) 263–290.
[48] A. Doucet, On sequential simulation-based methods for Bayesian filtering, Technical Report CUED/F-INFENG/TR.310(1998), Department of Electrical Engineering, University of Cambridge, UK, 1998.
[49] A. Doucet, S. Godsill, C. Andrieu, On sequential Monte Carlo sampling methods for Bayesian filtering, *Statistics and Computing* 10 (2000) 197–208.
[50] J. Ching, J.L. Beck, K.A. Porter, Bayesian state and parameter estimation of uncertain dynamical systems, *Probabilistic Engineering Mechanics* 21 (2006) 81–96.
[51] E. Lauga, T.R. Bewly, Performance of a linear robust control strategy on a nonlinear model of spatially developing flows, *Journal of Fluid Mechanics* 512 (2004) 343–374.
[52] A. Doucet, N. de Freitas, N. Gordon, *Sequential Monte Carlo Methods in Practice*, Springer, New York, 2001.
[53] C.S. Manohar, D. Roy, Monte Carlo filters for identification of nonlinear structural dynamical systems, *Sadhana, Academy Proceedings in Engineering Sciences, Indian Academy of Sciences* 31 (4) (2006) 399–427.
[54] C. Andrieu, A. Doucet, S.S. Singh, V.B. Tadic, Particle methods for change detection, system identification, and control, *Proceedings of the IEEE* 92 (2004) 423–438.
[55] A.F.M. Smith, A.E. Gelfand, Bayesian statistics without tears: a sampling–resampling perspective, *The American Statistician* 46 (2) (1992) 84–88.
[56] P.E. Kloeden, E. Platen, *Numerical Solution of Stochastic Differential Equations*, Springer, Berlin, 1992.
[57] G.N. Milstein, *Numerical Integration of Stochastic Differential Equations*, Kluwer Academic Publishers, Dordrecht, 1995.
[58] B. Oksendal, *Stochastic Differential Equations: An Introduction with Applications*, Springer, Berlin, 1992.